Available online at www.sciencedirect.com

jmr&t Journal of Materials Research and Technology

journal homepage: www.elsevier.com/locate/jmrt

Review Article

Fly ash-based adsorbent for adsorption of heavy metals and dyes from aqueous solution: a review

Uyiosa Osagie Aigbe [a,*], *Kingsley Eghonghon Ukhurebor* [b,*], *Robert Birundu Onyancha* [c,*], *Otolorin Adelaja Osibote* [a,*], *Handoko Darmokoesoemo* [d,*], *Heri Septya Kusuma* [e,*]

[a] *Department of Mathematics and Physics, Faculty of Applied Sciences, Cape Peninsula University of Technology, P.O. Box 1906, Cape Town, South Africa*

[b] *Department of Physics, Faculty of Science, Edo State University Uzairue, P.M.B 04, Auchi, 312101, Edo State, Nigeria*

[c] *Department of Technical and Applied Physics, School of Physics and Earth Sciences Technology, Technical University of Kenya, P.O. Box 52428–00200, Nairobi, Kenya*

[d] *Department of Chemistry, Faculty of Science and Technology, Airlangga University, Mulyorejo, Surabaya, 60115, Indonesia*

[e] *Department of Chemical Engineering, Faculty of Industrial Technology, Universitas Pembangunan Nasional "Veteran" Yogyakarta, Indonesia*

ARTICLE INFO

Article history:
Received 30 April 2021
Accepted 28 July 2021
Available online 9 August 2021

Keywords:
Adsorption
Fly ash
Nanosorbent
Wastewater
Nanotechnology

ABSTRACT

A critical global issue in the 21st century is water shortage, as well as its pollution with noxious metal ions and organic dyes. To extract these pollutants from wastewater, a variety of traditional methods have been employed but they lack reusability/recyclability, are expensive, environmentally unfriendly, unsafe and the remediation process takes a long time. Therefore, to treat these contaminants, nanotechnology (NT) has recently been granted several leeways in terms of making the desirable nanomaterials (NMs) with high surface-to-volume ratios and special surface functionalities. In particular, fly ash (FA) has stood out as one of the greatest exciting new-found affordable and high efficient materials for water decontamination owing to its high porosity, huge surface area, and exceptional features. Hence, this present review study will attempt to compile data from existing literature on the utilization of FA-based adsorbent for the removal of heavy metals (HMs) and dyes from wastewater. Based on the reviewed publications, Langmuir's isotherm models (LIMs) and Freundlich's isotherm models (FIMs) best described the sorption process thus signalling monolayer and multi-layer sorptions. Pseudo-second-order (PSO) model provided the best appropriate means in elucidating the kinetic process and both exothermic and endothermic processes revealed the nature of the thermodynamic process during sorption. Some recommendations in the form of future prospects on how to advance the capacity of the adsorption and effectiveness of FA on the removal of HMs, dyes and other environmental contaminants using innovative technologies such as the nanofiber technology is also been proposed.

* Corresponding authors.
E-mail addresses: uyi4we@gmail.com (U.O. Aigbe), ukeghonghon@gmail.com (K.E. Ukhurebor), 08muma@gmail.com (R.B. Onyancha), osibotea@cput.ac.za (O.A. Osibote), handoko.darmokoesoemo@gmail.com (H. Darmokoesoemo), heriseptyakusuma@gmail.com (H.S. Kusuma).

https://doi.org/10.1016/j.jmrt.2021.07.140

1. Introduction

Water is one of the amplest natural resources on the planet, nevertheless, only about 1.0% of it is useable for consumption by humans. Owing to the increasing costs of potable and clean water, rising populations, and several environmental and climatic issues, it is alleged that over one billion persons lack access to sufficient potable and clean water. The ongoing degradation of freshwater supplies by a combination of organic and inorganic contaminants is a major problem in the water supply chain [1].

Pollution of the air, soil, and water is a major problem in today's world, with the pollution of the water supply, in particular, raising serious concerns. Aside from a scarcity of water, the development of vast quantities of wastewater has placed a lot of strain on humanity [2]. The present growth of the population (overpopulation), innovation (in the form of modernization), industrial and economic development have both positive and negative consequences on the society, such as economic growth and contamination of the air, water, and soil. Water contamination is a serious concern because of its adverse effects on living organisms as well as the surrounding environment, and because it is generated in large quantities. Water sources such as the subsurface, lake, and river are increasingly depleting and being polluted as a result of global warming. Significant quantities of wastewater are inevitably generated by industrial, agricultural, and domestic activities [3,4].

The expansion of mining, smelting, biochemical/chemical industries, battery production, and the widespread utilization of biochemical/chemical substances for agricultural activities such as pesticides, herbicides and fertilizers results in a massive release of heavy metals (HMs) and dyes into the surface and groundwater [5]. Microorganisms, organics, and inorganics are the three primary types of pollutants found in water. Because of their toxicity to ecological and biological processes, heavy metals ions (HMI), which make up the majority of inorganic contaminants, have sparked a lot of concern [4]. As a result, scientists, water regulatory agencies, and government agencies are concerned about maintaining and improving water quality [6].

As a result, new-fangled technologies to reuse/recycle the produced wastewater are in high demand. Remediation and treatment of this produced wastewater is a core concern for developing countries, particularly when important factors such as reusability, recyclability, cost and sustainability are taken into account. HMs, especially those derived from the earth's crust, are difficult to degrade or eliminate [3].

Nanotechnology (NT) is thought to have the ability to shape our existing environment via the provision of new-fangled products, remediation/treatment methods, and sensors for environmental monitoring. There is a need for technology that can eliminate harmful pollutants from the atmosphere to a safe level and do so quickly, safely, and at a fair cost in the case of water purification. Thus, in the field of NT, the production of innovative nanomaterials (NMs) with improved affinity, power, and selectivity for HMs and other pollutants is a dynamic evolving aspect of research. These NMs can be utilized to increase water quality as well as the accessibility and viability of water supplies, for example, via advanced filtration, which allows for long-term water reuse, recycling, and desalination [7].

For adsorption, catalysis, electrostatic, reactivity and adjustable pore depth, sensors and optic-electronics with much characteristic ratio, aquaphobic (hydrophobic) and hydrophilic interactions, NT provide groundbreaking water treatment solutions. NT-based procedures are effective, flexible, and adaptable, allowing for high-performance and affordable water and wastewater treatment. Furthermore, NT can be used for cleaning and restoring rare water bodies at a low cost [8].

Due to the problems created by the inclusion of dyes and HMs in wastewater, traditional wastewater treatment techniques such as adsorption [9], coagulation [10], flocculation [11], precipitation [12], reverse osmosis [13], biological process [14], gamma radiations [15], and photocatalysis [16] have been used to remove them [2]. However, all of these approaches are costly, and when handling large volumes of water, adsorption

List of acronyms

AMD	Acid mine drainage
ARS	Alizarin red sorbent
BFA	Biomass fly ash
BKME	Bleached Kraft Mill Effluents
BBD	Box–Behnken design
BTB	Bromothymol blue
CA	Coal ash
CFFA	Coal-fired fly ash
Conc	Concentration
CR	Congo red
DA	Dye adsorption
USEPA	Environmental Protection Agency of the United States
ESS	Environmental sustainability and safety
FA	Fly ash
FIM	Freundlich's isotherm model
GI	Gastrointestinal
Gpolymer	Geopolymer
HM	Heavy metal
HMI	Heavy metals ion
IConc	Initial concentration (IConc)
LIM	Langmuir's isotherm model
MB	Methyl blue
MFA	Modified fly ash
MSWI	Municipal solid waste incineration
NM	Nanomaterial
NT	Nanotechnology
PFO	Pseudo-first-order
PSO	Pseudo-second-order
RSM	Response surface methodology
FAN	Treated fly ash
FAO	Untreated fly ash
WHO	World Health Organization
ZFA	Zeolite fly ash

procedures are favoured because of their benefits in terms of affordability, ease of operation, reliability, equipment simplicity, and most importantly, the adsorbent can be preferred from a wide range of natural, synthetic, and waste materials, such as fly ash (FA) [17]. Adsorption has long been utilized in industrial separation and purification procedures; there is currently increasing attention in adsorption employing other low-cost adsorbents. Adsorption occurs when a sorbent is cheap and prepared to use [18].

In several countries, new and/or stricter wastewater discharge regulations, as well as improved compliance, have been implemented in recent years. This problem has impelled extensive research into new innovative treatment methods, some of which are now being tested on a large scale. The removal of dyes and other organic matter, as well as HMs, from a procedure or waste effluent, has been shown to be highly effective using liquid-phase adsorption. There is currently increasing attention in employing affordable materials for dye and HMs adsorption [4]. Among different nanosorbent materials, FA is unquestionably a new research material, as confirmed by the trivial amount of published papers in indexed journals obtained from SCOPUS over the last ten years under the keywords "HMs and dyes removal using FA" (Fig. 1). As a result, the utmost aim of this study is to include a compilation of data from existing literature on the utilization of FA-based adsorbent for HMs and dyes removal from wastewater.

Subsequently, the remaining parts of this review study are planned as follow: Section 2 deliberates on HMs and dyes, Section 3 discusses FA-based adsorbent for HMs and dyes adsorption, Section 4 outlines some of the major factors affecting the adsorption process for HMs and dyes using FA-based adsorbent, Section 5 briefly discussed some of the utmost mechanism of adsorption using isotherms, kinetics and thermodynamics for HMs and dyes using FA-based adsorbent, Section 6 concisely deliberates on the regeneration and desorption process for HMs and dyes using FA-based adsorbent, while Section 7 is the last section containing the conclusion as well as some recommendations in the form of future prospect.

2. HMs and dyes

HMs are a form of persistent toxic material (PTS) that can cause acute toxicity and accumulation in living organisms. By entering the food chain, HMs have adverse effects on human health and the natural environment, climate inclusive. HMs are found naturally in the earth's crust, nevertheless, anthropogenic events have increased their content, resulting in ecological pollution [19]. Domestic, agricultural and industrial materials and activities such as fertilizer, batteries, alloy, textiles, sewage, biosolids, pesticides, pigments, steels, HMs, dyes, and wood preservation, electroplating and photographic materials are some of these anthropogenic sources [20]. High levels of toxic HMs such as chromium (Cr), lead (Pb), mercury (Hg), cadmium (Cd), and cobalt (Co) are discharged into the mainstreams of our drainage systems as a result of our cities' rapid industrialization and urbanization. These metals have higher stability and can harm our biodiversity and public health if they are released into the environment untreated [21]. HMs like Co, Cu, Cr, Fe, Mg, Zn, Se, Mn, Ni and Mo are considered important trace elements for physiological and biochemical work. Aside from these HMs, all other metals are recognized as non-essential. However, if these metals are present in excess of their tolerance value, they will damage the environment and human health [20].

HMs in wastewater are undesirable because of their solubility in water, which allows them to be ingested by living creatures, where they go into the food chain and begin to accrue in the human body [21]. HM has received unusual attention owing to its carcinogenic nature, its selective noxiousness even at low concentration and its lack of degradability. Over-exposure to these noxious HM can cause impairment of nerve, kidney, brain, liver, cardiovascular and endocrine systems and in grave circumstances, death. Given the detrimental impacts of HM, HM must be removed from liquefied wastes at acceptable regulation levels [22].

The potential human carcinogens based on epidemiological and experimental findings of the Environmental Protection Agency of the United States (USEPA) and the International

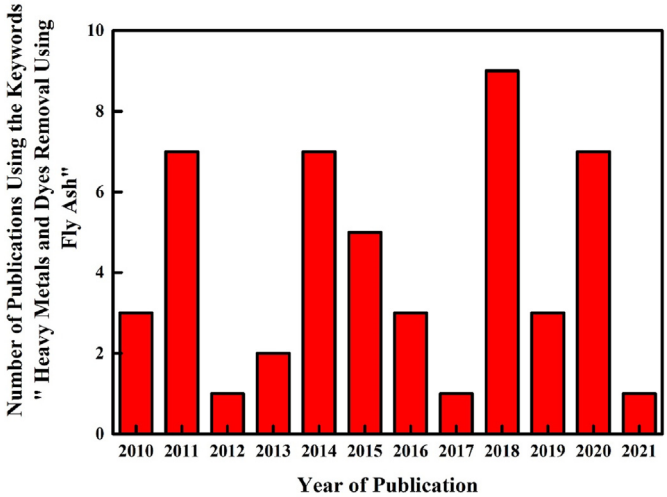

Fig. 1 – Illustration of the number of publications using the keyword "heavy metals and dyes removal using fly ash" published from 2010 to 2021 obtained from "SCOPUS".

Table 1 – Summary of several toxic metals, their effects and recommended allowed levels in water.

HMs	Impacts of HMs	Recommended Allowed Levels by USEPA and WHO	References
Pb	Anaemia, brain mutilation, anorexia, malaise, lack of appetite, liver, kidney, gastrointestinal mutilation, mental retardation in infants, and nervous system disorder	15 ppb	[4,24,25]
Ni	Chronic bronchitis, reduced lung function, lung cancer, contact dermatitis, cardiovascular disease, asthma, lung fibrosis, and respiratory tract cancer	0.02 mg/L	[25,26]
Cr	Epigastria pain nausea, vomiting, severe diarrhoea, producing lung tumours	100 ppb	[4,25]
Hg	Damage to the nervous system, protoplasm poisoning, corrosive to skin, eyes, muscles, dermatitis, kidney damage, and gastrointestinal (GI)	1 mg/L	[24,25]
Cu	Neurotoxicity, and acute toxicity, dizziness, diarrhoea	1300 ppb	[4,25]
Cd	Damage to the kidneys, respiratory systems, and skeleton.	0.005 mg/L	[27,28]
As	Causes cancers of the urinary tract, bladder and skin, bronchitis, dermatitis, bone marrow depression, haemolysis, and hepatomegaly	10 mg/L (WHO)	[24].
Zn	Causes short term metal-fume fever, gastrointestinal distress	3.0 mg/L	[25,29]

Agency for Research on Cancer (IARC) are Hg, Cr, Cd, As and Pd [20]. An outline of various HM, their impacts and their recommended allowed limits of various HMs in drinking water according to the World Health Organization (WHO) and the USEPA in Table 1. Some metals such as As, Cd, Cr, Hg and Pb are characterized under metals of utmost interest and are critical to community health; due to their high-level harmfulness, various organ impairment driven by the exposure even at minimal concentration [20,23].

Only a few metals, such as Cu and Zn are needed in small quantities for the human body's metabolism to function properly. However, higher concentrations of non-biodegradable HMs such as Fe, Cr, Pb, As, Ni, Cd, Se, and Hg in their numerous oxidation states in living creatures (humans, animals and plants) cause serious health and environmental issues [3].

Over ten thousand dyes are utilized in the textile industry today, with more than 280,000 tonnes (t) being discharged annually globally [30]. The discharged textile effluents are full of dyes, radioactive metals, infectious pathogens and parasites, suspended solids, biodegradable, unstable, and intractable organic composites. Textile industry effluents alter the biotic/natural life of the aquatic environment (rivers and lakes). Dye loaded wastewater damage the ecosystem by posing a threat to groundwater supplies. These wastewaters are brightly coloured, have a changing pH, a high temperature and chemical oxygen demand, and contain a significant amount of suspended oils. The key issue with dyes in wastewater (which are light stable but not biodegradable) is the colour, which reduces light penetrability and thus has an undesirable impact on photosynthesis. The amount of oxygen decomposed, as well as the decreasing permeability of light, result in the extermination of certain living creatures and the constraint to water reuse [21].

Various products such as azo-, antrachinone-, thiazine-, and metal-complex dyes are recognised for their high noxiousness, with some of them being carcinogenic, non-biodegradability, and accumulate in plants, livestock, and humans, dyes are the most common contaminants in wastewater. The composition of dye wastewater is becoming increasingly complex as the diversity of industrial goods grows, and its treatment has become an extremely difficult task [30,31]. Many parameters in the textile industry effluents are highly variable, including BOD, turbidity, colour, COD, pH, odour, and salinity. Because of their toxicity, mutagenicity, and carcinogenicity, azo dyes such as congo red (CR), Direct Blue15, and Direct Red 2 are known to cause health problems [32].

HMs derived from dye structure are also a concern. They can be utilized as catalysts during the production of certain dyes and as impurities or as part of the dye particles, establishing an essential structural element. HMs in wastewater are undesirable because of their solubility in water, which allows them to be ingested by living creatures, where they go into the food chain and begin to accrue in the human body [21]. Since synthetic dyes are linked to other contaminants in textile finishing industry effluents, efficient elimination procedures should aim not only the colour elimination but also the other composites such as HMs, surfactants, pH-conditioners, whitening agents, etc. that are present in dyeing and rinsing baths [30]. As a result, removing these pollutants from wastewater is important to make it reusable [3].

3. Fly-ash based adsorbent for heavy metals and dyes adsorption

Electricity accounts for a significant portion of global energy demand. As reported by the "International Energy Agency (IEA)", the overall average gross electricity output in 2018 was 26,700 TWh, a 3.8% increase over gross energy production in 2017. Despite the widely discoursed on the negative environmental consequences of coal use, it continues to be the world's largest source of energy. The burning of coal and biomass in thermal power plants produces massive quantities of ash residues. Globally, approximately 750 million tons of coal ash (CA) and 480 million tons of biomass ash are generated yearly, according to conservative estimates [33].

FA is a large solid waste constituent released by coal-fired thermal power plants used to generate electricity and produces 600 million tonnes of FA per year globally. The temperature of the combustion process reaches 2000 °C. At such

high temperatures, the majority of the inorganic material in coal melts and fuses [4,34,35]. The chemical structure of FA is determined by the form of coal used and the temperature at which it is burned. The main constituents of FA are alumina (Al_2O_3), hematite ($\alpha - Fe_2O_3$), silica (Si), calcium (Ca), magnesium (Mg), sodium (Na), potassium (K), and titanium oxides (TiO_2). Hg, Cd, As, Co, Cu, Pb, Cr, and other HMs contribute to the toxicity of FA [4].

The physiochemical natures of ash residues formed during coal and biomass combustion differ significantly. CA is also made up of spherical particles. The chemical structure of FA is determined by the form of coal used in the burning process (bituminous, sub-bituminous, or lignite). According to the "American Society of Testing and Materials (ASTM C618)", CA residues is divided into two categories based on their chemical composition: "Class F and Class C". The combined SiO_2, Fe_2O_3, and Al_2O_3 contents of Class F ash residues are greater than 70.0%, and these residues have a low lime content. The content of SiO_2, Fe_2O_3, and Al_2O_3 in Class C ash residues ranges from 50 to 70%, and these residues are high in lime. Biomass ash residues, on the other hand, are divided into two categories: FA and bottom ash. The FA is made up of fine constituent parts that rise with the flue gases, while the bottom ash is made up of bigger constituent parts that accumulate at the furnace's bottom. The particles in both forms of biomass ash residues are irregular in form. The bottom ash is primarily composed of SiO_2, with varying amounts of other elements such as Al_2O_3, Fe_2O_3, CaO, K_2O, Na_2O, and MgO. FA, conversely, may contain vast amounts of plant matter [33].

FA is a powdery material made up primarily of spherical, porous, and amorphous particles. Bituminous FA has a particle size of less than 0.075 nm. Sub-bituminous coal FA, on the other hand, is rougher and larger than bituminous coal FA. The basic gravity of most FA is between 2.1 and 3.0, but the surface area varies widely between 170.0 and 1000.0 $m^2\ kg^{-1}$.

Table 2 – Properties of FA [4].

FA Feature	Characteristic Value
Colour	Greyish white
Average size of the particle (μm)	10–100
Specific gravity	2.1–3.0
Bulk density (g/cm^3)	0.90–1.70
Permeability (cm/s)	15–39
pH	6–8

The carbon content gives the FA a blackish hue. While the chemical properties of FA are heavily influenced by the methods of handling and storage, as well as the composition of coal. Anthracite, bituminous, sub-bituminous, and lignite coal are the different types of coal. Lignite and sub-bituminous FA have higher CaO and MgO content, lower silica and magnetite concentrations, and lower unburned carbon content than bituminous FA. Only a limited amount of anthracite FA is available because anthracite is the purest type of coal that is not burned in thermal power plants. Tables 2 and 3 show the FA properties and typical chemical composition spectrum of their different forms [4,36].

In 2015, the demand for FA was worth US$ 39,548.1 million and is projected to hit US$ 64,761.9 million by 2022, rising at a CAGR of 7.3 percent from 2016 to 2022 (Fig. 2) [37].

On the other hand, global FA use is just around a quarter of total output (Fig. 3), with Europe leading the way with a value of 47.0%, followed by the United States with a value of 39.0%, and unused FA is usually contained in ash ponds or surface impounding. These impounding are large open lands that can hold some billion of tons of FA, raising concerns about pollution both below ground (water bodies) and above ground (air). Given the imminent strict disposal citing constraints, declining landfill space availability, and rising disposal costs, FA utilisation technologies that are both cost-effective and environmentally friendly are needed. Furthermore, maximizing FA reuse rather than storage and disposal is the best way to alleviate environmental issues while also creating new economic opportunities. Just about a quarter of a percent of FA is used in soil amelioration, Portland cement, ceramic, zeolite, and fiber processing, catalysis, fillers in polymers, and adsorbents in wastewater treatment [38].

As a result, it has been used as a cement additive (due to its pozzolanic property), concrete, in brick manufacturing, as a backfill material, as a reinforcing filler in polymers, highway embankment, as a composite material, as an adsorbent for gases and contaminants from wastewater and as soil ameliorant in recent decades. FA has also been regarded as an ideal precursor for the synthesis of zeolites and geopolymer (Gpolymer) due to its high silica and alumina content. Because of the significant disposal issues, which pose environmental risks such as heavy metal cation leaching into soils and groundwater, the efficient use of FA has drawn international interest [35,39]. Hence, repurposing it as an adsorbent in the elimination of various forms of contaminants from effluent

Table 3 – Chemical properties of various FA [4].

Component (wt%)	Bituminous	Sub-bituminous	Lignite	Anthracite
SiO_2	20.00–60.00	40.00–60.00	15.00–45.00	43.50–47.30
Al_2O_3	5.00–35.00	20.00–30.00	10.00–25.00	25.10–29.20
Fe_2O_3	10.00–40.00	4.00–10.00	4.00–15.00	3.80–4.70
CaO	1.00–12.00	5.00–30.00	15.00–40.00	0.50–0.90
MgO	0–5.00	1.00–6.00	3.00–10.00	0.70–0.90
SO_3	0–4.00	0–2.00	0–10.00	–
Na_2O	0–4.00	0–2.00	0–6.00	0.20–0.30
K_2O	0–3.00	0–4.00	0–4.00	3.30–3.90
S	0.08–0.67	0.70–0.90	–	0.10–0.50
TiO_2	0.50–1.00	1.10–1.20	0.20–0.60	1.50–1.60
LOI	0–15.00	0–3.00	0–5.00	8.20

Fig. 2 – Global market revenue and growth of FA [37].

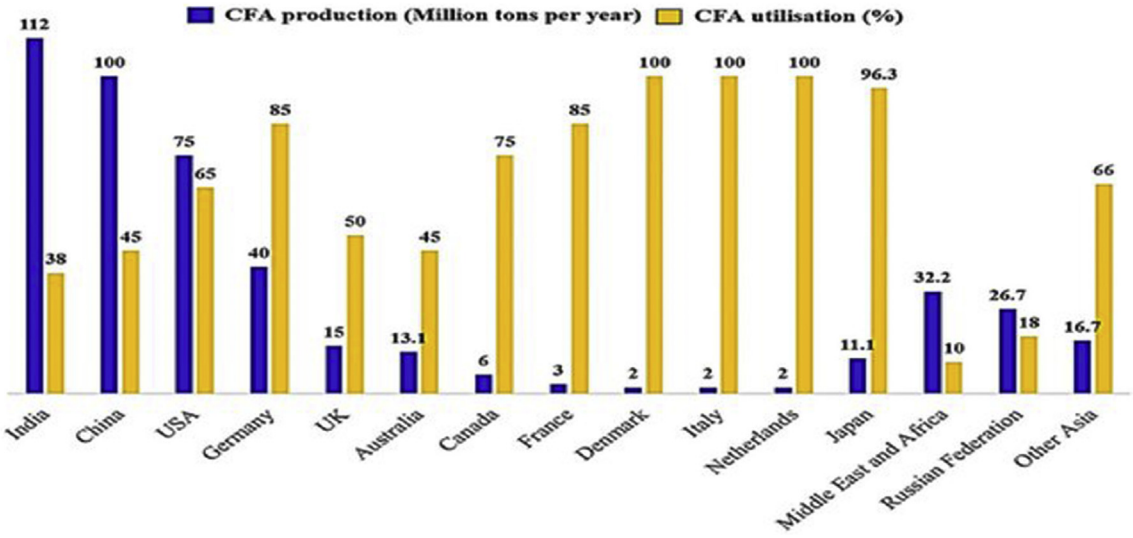

Fig. 3 – Global production and use of FA [38].

addresses two issues for waste management and water quality [17].

FA is a strong and low-cost adsorbent for HMs and dyes due to its surface structure, charge, and morphology. As a result, FA, either alone or in combination with photocatalysts is a complex substrate capable of simultaneously removing HMs and dyes. Regulated surface charge and huge specific surfaces are needed to improve the efficiency of the process. The crystallinity and surface energy of raw FA can be altered. Surfactants aid morphology control by increasing pore sizes on the adsorbent material as the length of the surfactant's tail, pH, and post-synthesis temperature increase [30].

A cost-effective sorbent zeolite Linde type A (LTA) synthesized from coal FA (CFA-ZA) was employed for Hg(II) elimination using an industrial effluents matrix. The average removal efficiency of 94% was noticed using CFA-ZA for Hg(II) confiscation and the sorption process was best depicted employing the FIMs and the pseudo-second-order (PSO) model. The observed sorption capacity was 0.44 mg/g and the chemisorption and physisorption were suggestive of Hg(II) ions sorption onto the surface of CFA-ZA [40].

A novel magnetic Schiff's based-chitosan-glyoxal/FA/Fe_3O_4 (Chi-Gly/FA/Fe_3O_4) NCs prepared by the direct composition of magnetic Chi with FA powder particles and the subsequent crosslinking reaction of Gly with Schiff's base formation (Fig. 4) was employed in the removal of reactive orange 16 (RO16).

The impact of various sorption parameters was enhanced utilizing the Box–Behnken design (BBD) in the response surface methodology (RSM). According to the surface analysis of Chi-Gly/FA/Fe_3O_4, the surface area of the sorbent was 3.31 m^2/g, and a mean opening diameter of 14.5 nm and a total opening volume of 0.012 cm^3/g. Also according to the IUPAC classification, the nanosorbent was a mesoporous material. While the surface morphology structure of the sorbent before and after sorption of RO16 are shown in Fig. 5. Fig. 5 (a and b)

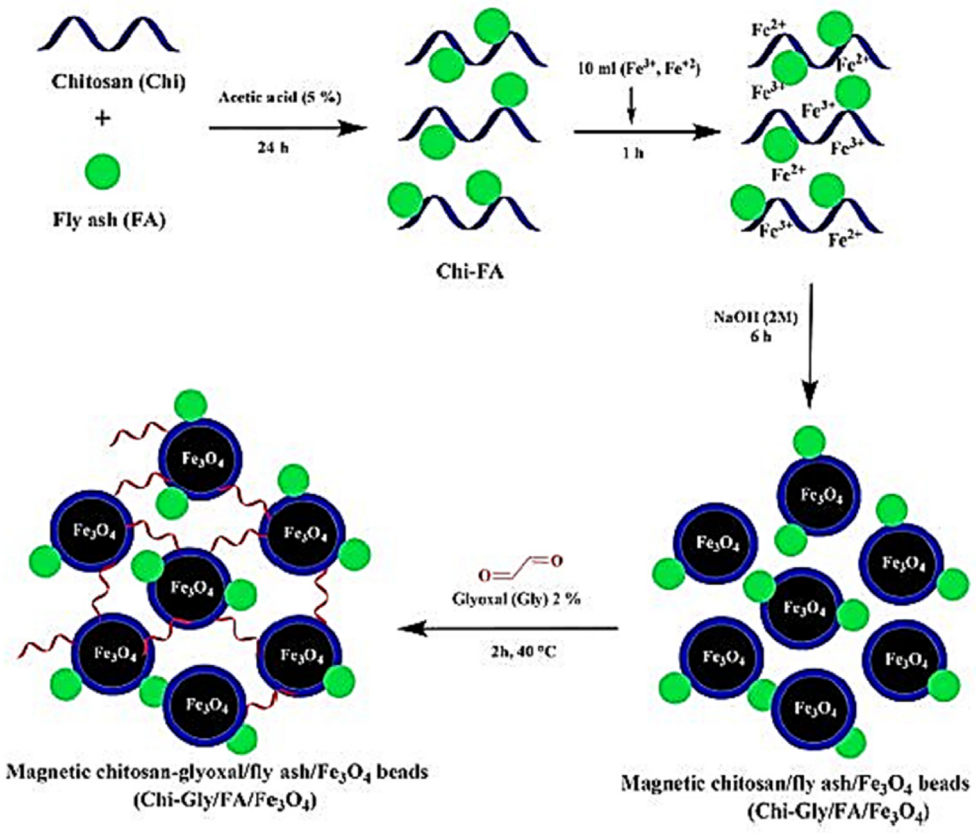

Fig. 4 – The steps of Chi-Gly/FA/Fe_3O_4 preparation [41].

shows the SEM image and EDX analysis of the nanosorbent, with a rough, porous comprising crevices and cracks. While the EDX analysis before sorption of RO16 confirms the elementary composition of the nonabsorbent to contain Fe, C, O, N and Zr. After sorption of RO16, there was a more compact evanescence of cervices on the surface of the nanosorbent, indicative of the molecules of RO16 sorbed to the nanosorbent. The presence of the S element was observed after the sorption of RO16 onto the nanosorbent from the EDX analysis.

The optimal elimination of RO16 was observed at 4.0, with a percentage removal of 96.2%. This was attributed to the electrostatic interface between the protonated amino (NH_3^+) functional group of the sorbent and the sulfonate (SO_3^-) group of the dye as depicted by Eq. (1).

$$R-NH_3^+ + RO16-SO_3^- \leftrightarrow R-NH_3^+ - -SO_3^- - RO16 \quad (1)$$

The sorption process was also noticed to follow the PSO and FIMs, with a determined sorption capacity of 112.5 mg g^{-1}. The sorption mechanisms were ascribed to the electrostatic, n-π, H-bonding, and Yoshida H-bonding interactions [41]. 3-aminopropyltriethoxy silane (APTES) was utilized to functionalize biomass FA (BFA) to create low-cost and effective sorbents using a simple chemical modification method for the sequestration of anionic dyes. The SEM images in Fig. 5, shows the structural morphology of BFA and BFA-APTES. The sorbents revealed heterogeneous (mixed) surface features with macropores of diameter greater than 50.00 nm and particles of various sizes ranging from 20.00 to 500.00 nm. The surface treatment did not affect the micropore size as depicted in Fig. 6 (a, and d) and while there was almost an order of size reduction in the size of the constituent parts (Fig. 6 c and f).

The optimal percentage removal for both dyes (alizarin red S (ARS) and bromothymol blue (BTB)) at a pH range of 2.0–12.0 were pH 2.0 and 4.0 using respective sorbents, which was ascribed to the electrostatic interaction between the positive charged BFA-APTES and the anionic dye ARS and BTB. The determined sorption dimensions of BFA-APTES for BTB and ARS were 15.44 and 13.42 mg/g, which were 2–3 times greater than the values obtained using pristine BFA. While from the thermodynamics parameters, the sorption of ARS and BTB was found to be spontaneous and exothermic using BFA-APTES [33].

While in the study of Liu et al. [42], a comparative study of FA, FA-based Gpolymer and faujasite block altered from Gpolymer were evaluated for the elimination of Pb(II). The sorption of Pb(II) onto Gpolymer and faujasite block and FA were best describe using the PSO and pseudo-first-order (PFO) and the LIMs. The determined sorption capacity using these sorbents were 49.80, 118.60 and 143.30 mg g^{-1} at pH values of 3.0 for FA, Gpolymer and faujasite respectively.

In this study, municipal solid waste incineration (MSWI) FA was modified using the microwave-assisted hydrothermal process to obtain zeolite and which was used to treat wastewater contaminated with HMs (Cu, Cd, Mn, Ni, Pb, and Zn).

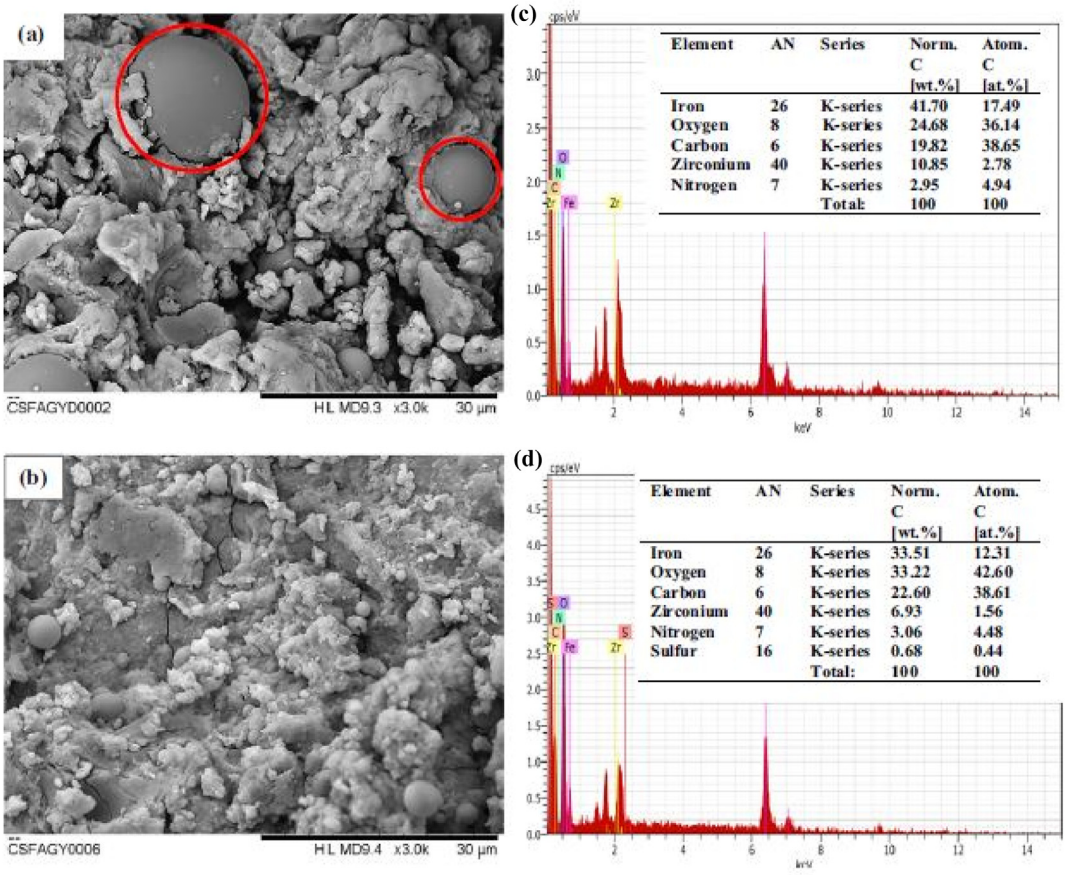

Fig. 5 – (a and b) SEM image and EDX of Chi-Gly/FA/Fe_3O_4 before sorption and (c and d) SEM image and EDX of Chi-Gly/FA/Fe_3O_4 after sorption [41].

The optimal pH value for the elimination of the individual HM was 2.0 and the sorption processes were best described utilizing the PSO and LIMs. The determined sorption capacities were 10.58 (Cd), 27.55 (Cu), 15.46 (Mn), 13.61 (Ni), 50.00 (Pb) and 20.16 mg/g (Zn) [43].

SBA-15 mesoporous molecular sieves were created from FA employed in a thermal plant in Inner Mongolia in China employing the alkali two-steps hydrothermal techniques. The synthesized SBA-15 were utilized for the Pb(II) removal. It was observed from the TEM images in Fig. 7, that the sorbents had

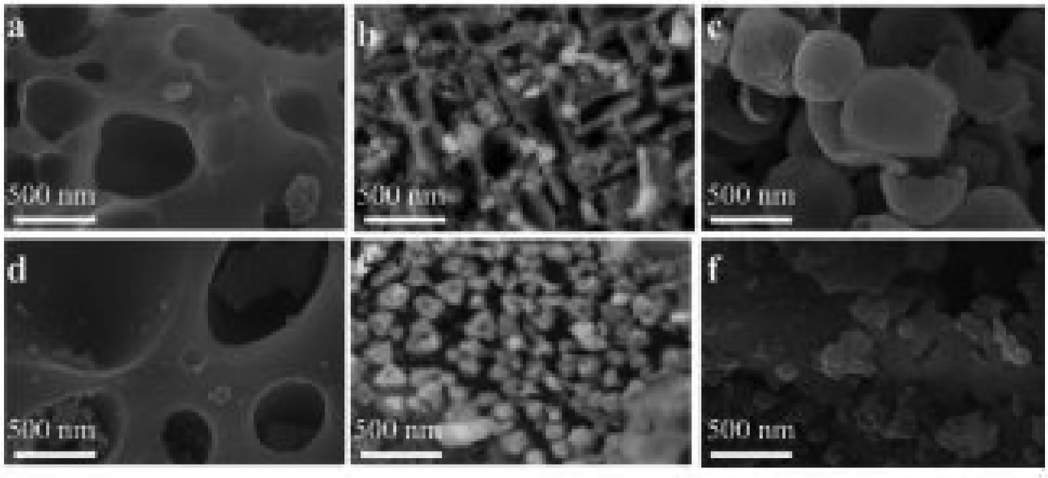

Fig. 6 – SEM images of various sizes before functionalization of BFA (a–c) and after functionalization to create BFA-APTES (d–f) [33].

a characteristic 2-D hexagonal pore structure, with mesoporous pore size range and pore thickness of 5–7 and 3 nm.

Also, it was noticed that the confiscation efficiency was gradually improved with growing contact time, temperature and IConc of Pb. The optimal elimination rate of 98.0% was noticed at a pH value of 5.0. The PSO and the LIMs best defined the sorption of Pb(II) to the sorbent and with an uppermost sorption capacity of 131.0 mg·g^{-1} [44].

Nguyen et al. [45], produced a characteristic FA modified using 2- mercaptobenzothiazole (MBT) and sodium dodecyl sulfate (SDS) as the surfactants after treating with 1.0 M NaOH solution, which was employed for the elimination of Cd(II) and Hg(II). The FESEM images shown in Fig. 8, depict FAO and FAN particles before and after functionalization, It was observed that the particles of FA had a spherical shape with a particle diameter range of 100–10 μm. But the key size of the particle is within 3–5 μm. The particles of untreated FA (FAO) has a smooth surface in comparison to the treated FA (FAN) and modified FAN (FASDS and FAMBT) which had a rough surface. The sorption isotherm models that best describe the sorption process of Cd(II) and Hg(II) were LIMs and FIMs, with the determined sorption capacity were 12.4 and 1.91 mg g^{-1} for Cd(II) and Hg(II).

Modified FA (MFA) was prepared by [45], using a 2-phase technique involving oxalic acid reduction, was used for the elimination of Cr(VI). The PSO and LIMs best define the sorption of Cr(VI) to the modified FA and the maximum sorption capacity was 12.34 mg/g [46].

While FA containing an elevated unburnt carbon was functionalized using alkali hydrothermal treatment. The synthesized modified FA was explored for Al, Fe, Ni, Pb, Mn and Zn from acid mine drainage (AMD) removal. As observed in the photomicrographs images in Fig. 9, the FA contained a very fewer amount of cenospheres created as a result of the condensation of the aluminous and siliceous droplet in air, which encompassed asymmetrical, porous "sponge-like"

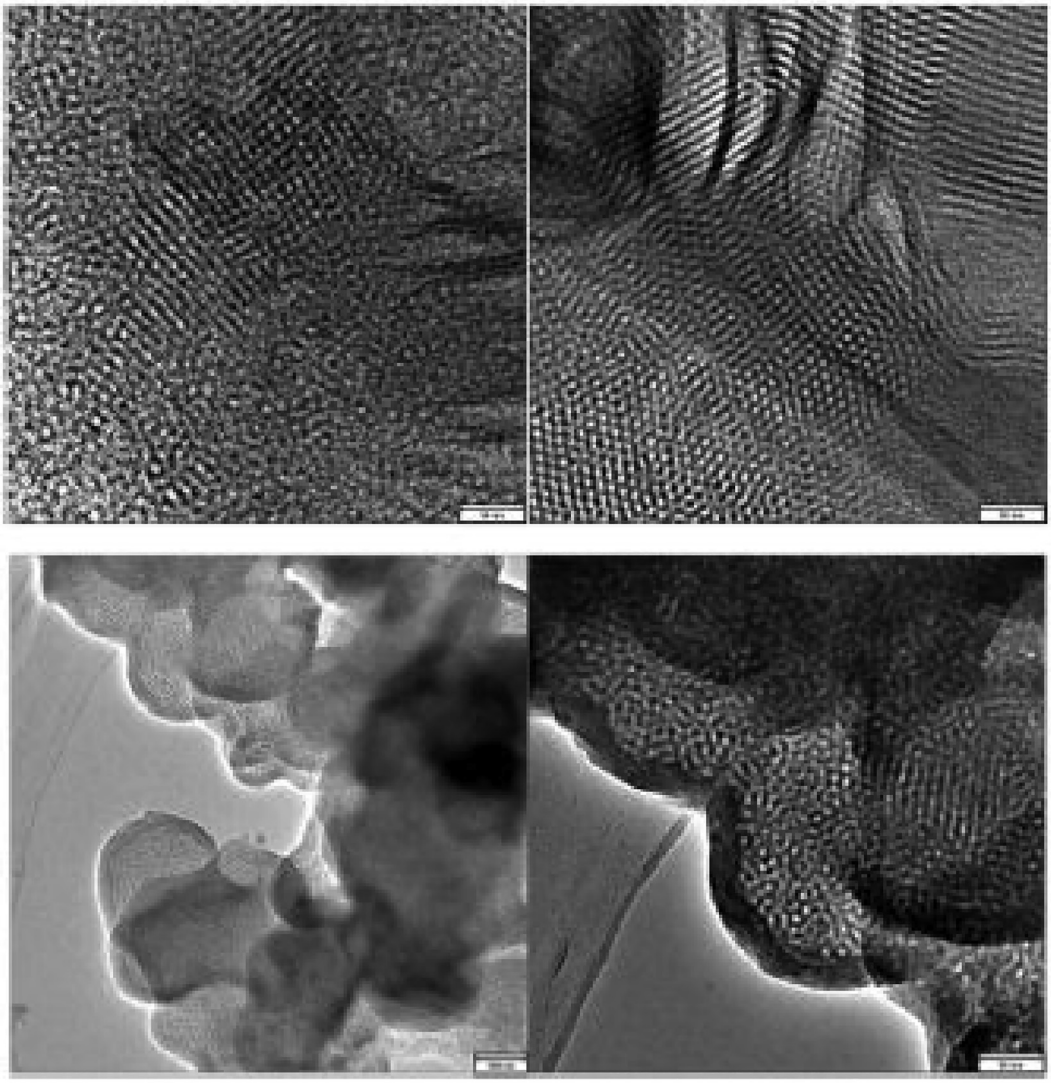

Fig. 7 – TEM images of SBA-15 [44].

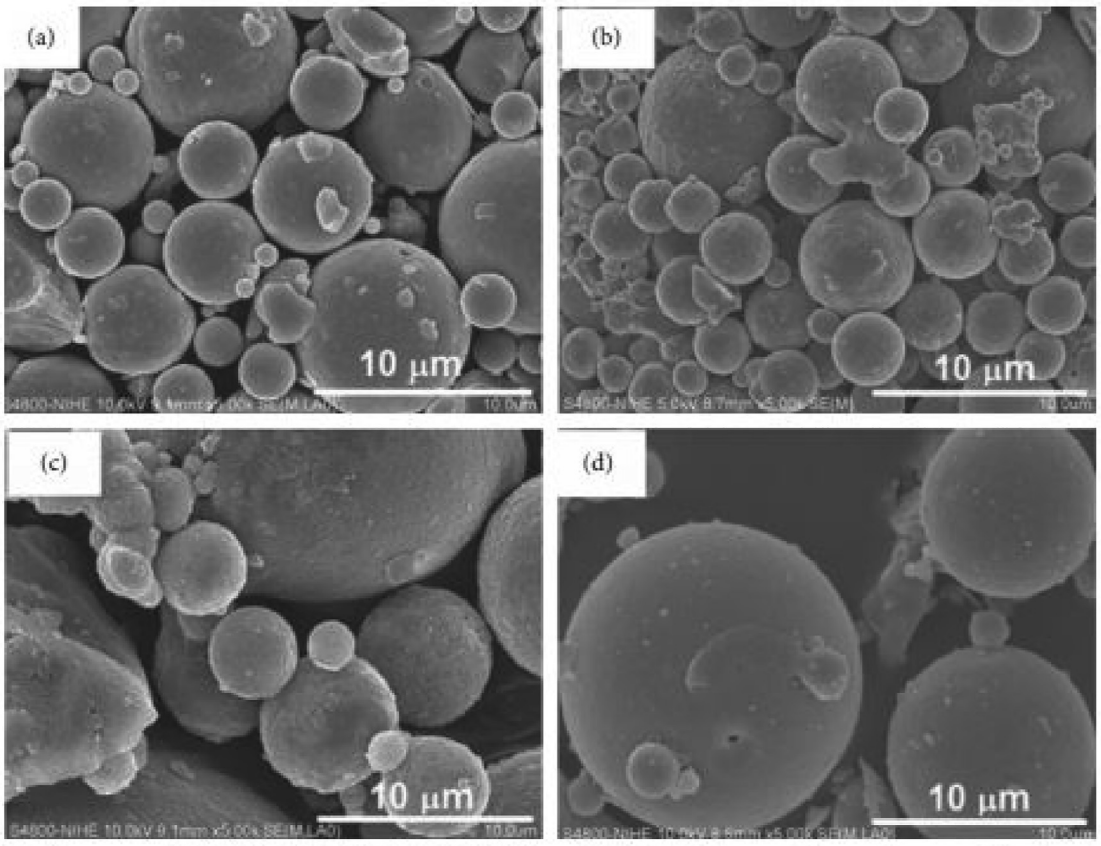

Fig. 8 – FESEM images of (a) FAO, (b) FAN, (c) FAMBT, and (d) FSDS particles at 5000 times magnification [45].

constituent parts of unburned carbon, which were assembled in the coarser portion (Fig. 9a).

The sorption of the various HMs onto MFA was at a first swift, which subsequently decelerated. The ideal duration for the uptake of HMs using an optimal dose of MFA of 120.0 g L^{-1} was 180 min, while the FIMs best define the sorption of these metals onto MFA, indicating that the sorption procedure was controlled by the sorbent heterogeneous (mixed) nature. Also, the PSO model best described the sorption process of most HMs to MFA, indicating that chemisorption is the sorption rate-limiting step and Mn is described by the intra-particle diffusion [47]. Based on the experimental results from previous studies reviewed, FA is promising sorbents for the removal of HMs ions and dyes molecules. A list of FA utilized in the sorption of different HMs and dyes with their optimum pH, isotherm and kinetics models, thermodynamics and sorption capacity values are summarized in Table 4. The capacities of adsorption of the FA-based adsorbents as shown in Tables 4 and 5 indicate that a relatively high acceptance capacity of HMI and dyes was observed, indicating that FA-based adsorbents are suitable for the elimination of HMs and dyes from effluent.

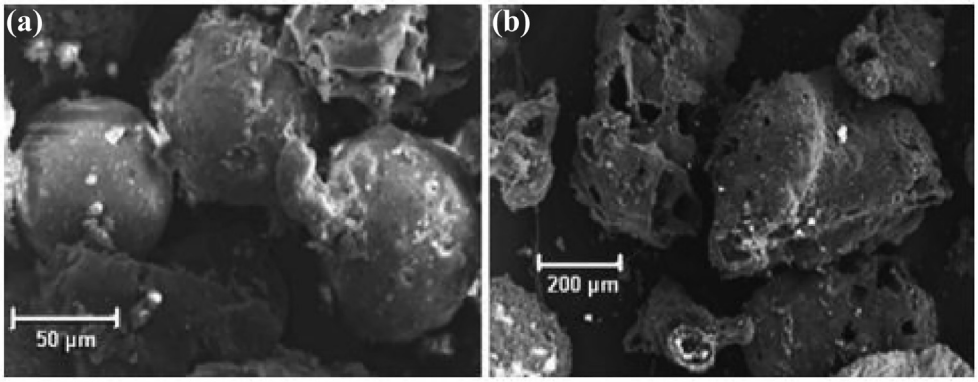

Fig. 9 – The photomicrographs of (a) cenosphere and (b) porous structure of FA [47].

4. Factors affecting the adsorption process of HMs and dyes using FA-based adsorbent

The adsorption process of HMs and dyes occurs through the exchange of ions, coordination, chelation, complexation, the combination mechanism, microprecipitation as well as the interaction of the electrostatic forces [73].

The adsorption process is considered by some adsorption circumstances (such as the pH, temperature, time of contact, adsorbent dosage, IConc, volume treated, the size of the particles, the types of adsorption system, and co-existing ions on the absorption process), the absorbent physicochemical features (such as the chemical, biochemical, and the ability or functionality of the texture) as well as the possessions of the sorbate [9,12,73].

Some of the reported utmost factors that affect the adsorption process of HMs and dyes are the pH, temperature, time of contact, adsorbent dosage, IConc, volume treated, the size of the particles, the types of adsorption system, and co-existing ions on the absorption process; these factors greatly influence the performance of the NMs for the elimination of HMs and dyes [5,74,75].

The adsorption procedure of HMs and dyes using FA-based adsorbent as well as other adsorbents have been considered and understudied by several researchers as one of the vital aspects in the decontaminating and removal process that has yielded several beneficial results in dealing with HMs and dyes, especially as it relates to environmental sustainability and safety (ESS) issues; all these are gear toward proffering solutions to the environmental contamination tenacities which has been reported as one of the global prime problems confronting the entire ecosystem [11,42,73].

According to Darmayanti et al. [73], owing to the properties of the FA and the circumstances employed in the adsorption procedures, the decontaminating and removal efficacies of HMs and dyes using FA as adsorbent changes; this indicates that these adsorption processes of HMs and dyes using FA-based adsorbent are mostly influenced by some major factors (circumstances) such as pH, temperature, time of contact, adsorbent dosage, IConc and co-existing ions on the sorption process. Hence, this section attempts to present, explore and concisely discuss some of these major factors or circumstances (such as pH, temperature, time of contact, adsorbent dosage, IConc and co-existing ions on the sorption process) affecting the adsorption process of HMs and dyes using FA-based adsorbent drawn from existing literature. Reportedly, these influences or effects also depend on some mechanism of the adsorption processes such as the isotherm and kinetic models as well as the thermodynamics discussed in Section 5 [9,11,12,76].

4.1. *Effect of pH*

One of the most critical variables and regulatory parameters in the adsorption procedures of HMs and dyes is pH. The pH not only influences the adsorbents surface charge, but also the extent of the ionization and sorbate speciation throughout the adsorption process [43,73,77]. The pH solution influences not just the surface charge of the prepared ingredients but also modifies the distribution of HMs; thus, resulting in the interaction of the electrostatic forces between the effluent (wastewater or pollutants) and the new-fangled NMs [78].

Consequently, Darmayanti et al. [73], reported that pH is one of the foremost determinants (dependants) in the adsorption process of HMs and dyes from effluent (wastewater) and other environmental contaminants using FA-based adsorbent. Also, the pH influences the charges on the surface of the adsorbent, the degree (magnitude) of ionization, and speciation (determination) of the adsorbate [73,79].

As reported by [73], the adsorption of HMI from the effluent is mostly dependent on the pH. In their study, they reported that the removal proportion of Cu^{2+} ions due to the pH values ranging from 3.0 to 8.0 at a concentration of 100.0 mg Cu/l and a FA dosage of 10 g/L; the adsorption of the Cu^{2+} ions raised in proportion with the pH and rapidly reached about 90.0% and 50.0% removal at a pH value of 5.0 and 6.0 for the used first FA (FA1) and second FA (FA2) respectively (Fig. 10).

The consequence of the pH on the Pb^{2+} ions and Cu^{2+} solutions on the uptake degrees of the Pb^{2+} ions and Cu^{2+} ions by FA was undertaken in a pH ranging from 4.0 to 12.0. The degree of uptake of these metal ions (Pb^{2+} ions and Cu^{2+}) by the FA was reported to have increased generally. However, these increments were in a non-progressive pattern, especially at high pH values. The consequence of the temperature on the uptake of these HMI (Pb^{2+} ions and Cu^{2+}) was examined at a temperature ranging from 30.0 °C to 60.0 °C, the adsorption of these HMI (Pb^{2+} ions and Cu^{2+}) was observed to be more enhanced at the lower temperature values. They also reported the constants' rate (k) in terms of first-order kinetics, and the k uptake of Pb^{2+} was approximately 1.80×10^{-2} s^{-1} and that for Cu^{2+} was approximately 2.10×10^{-2} s^{-1}. In all, their experimental results highlight the possibility of coal FA for the elimination and recovery of HMI from effluent.

The removal features of Pb^{2+} ions and Cu^{2+} ions from aqueous solution using FA-based adsorbent was examined by Alinnor [75], under several circumstances such as the pH, the time of contact and the temperature. The consequence of the pH of the HMI media on the acceptance levels of the HMI by FA was carried out within a pH ranging from 4.0 to 12.0 with a maximum adsorption capacity of 21.0 mg/g. The extent of acceptance of Pb^{2+} ions and Cu^{2+} ions by the FA was largely amplified, but at higher values of the pH; implying that the pattern is not in a progressive one. The influence of HMI adsorption on the pH was not the same for the two studied HMI (Pb^{2+} and Cu^{2+} ions); accordingly, the HMI adsorption on the oxide surfaces is connected to the hydrolysis reaction that was experienced in solution. Hence, the divalent HM cations in aqueous solution hydrolyze according to Eq. (2):

$$M^{2+}(aq) + nH_2O = M(oH)^{2n} + nH^{+} \quad (2)$$

where. $M^{2+} = Pb^{2+} or\ Cu^{2+}$.

The consequence of the pH on the adsorption of Pb^{2+} ions on FA, Gpolymer and faujasite was carried out by Liu et al. [42], where they reported that the adsorption efficiencies of faujasite, FA and Gpolymer all rise as the pH value rises in the elimination of Pb^{2+} from aqueous solutions; at higher pH values ranging from 4.0 to 6.0, that was when the increase in the quantity HM ions adsorbed on these absorbents'

Table 4 – A summary of HMI and dye removal using FA related sorbents.

Adsorbent	Contaminant	Optimum pH	Adsorption Time (Min)	Maximum Sorption Capacity (mg/g)	Isotherm	Kinematics	Thermodynamics	References
FA	Sulfate	8	5	146.1	FIMs	PSO	–	[23].
FA	Ammonium	8	60		FIMs	PSO	Exothermic.	[48].
chitosan/FA composite	Cr(VI)	5	50	33.27	LIMs		Exothermic	[49].
FA-based adsorbents (FA-ZA and FA-ZX)	Methyl blue (MB)	–	–	19.59	LIMs	PSO	Endothermic	[50].
Acid-modified FA (MFA)	Phosphate	7	60	13.3 $mgPg^{-1}$	LIMs	PSO	Endothermic	[51]
FA	Cu(II)	4.4	30	221	FIMs	–	Chemical ion-exchange	[52]
Chitosan/NaOH/FA composites	Tannic acid	5.5		243.90	Redlich-Peterson	PSO	Exothermic	[53]
alumina-silica nano-sorbent FA	Ni(II)	7	–	49.754	LIMs	PSO	Exothermic (low temperatures) and endothermic (high temperatures)	[54]
Zeolite (ZFA) prepared from FA	Cr(VI)	6	240	37.4	LIMs and FIMs	PFO (at high initial) PSO at lower initial concentration (IConc)	Endothermic	[55]
Porous Gpolymer-based FA	Cu(II)	6	–	113.41	LIMs and FIMs	–	Endothermic	[56]
FA	Pb(II)	6.2	60	51.98	FIMs	PSO	–	[57]
FA coated by chitosan (FAICS)	Cr(III,VI), Cu(II), Zn(II) and As(V)	4, 4, 6 and 6	180	36.22, 28.65, 55.52, and 19.10	FIMs	PSO	Endothermic	[58]
NaP zeolite adsorbent synthesized from coal FA	Zn(II)	5	120	39.96	LIMs	PSO	Endothermic	[59]
Microwave-assisted alkali-modified FA	Hg(II)	–	90	2.6663	LIMs	PSO	–	[60]
Hybrid FA composites	dye	6	40	24.8	LIMs	PSO	Exothermic	[61]
FA-based Gpolymer	Cu(II)	6	–	152	LIMs	PSO	Endothermic	[62]
FA-based Gpolymer (FAGP)	anionic surfactant SDBS	2	180	714.3	LIMs	PSO	Endothermic	[63]
FA-based Gpolymer	Pb(II)	5	120	84.5	LIMs		Endothermic	[64]
FA leachate	Pb(II)	6	30	349.7	LIMs	PSO	–	[65]
FAU-type zeolites prepared from coal FA	Pb(II), Cu(II), Cd(II), Zn(II), and Co(II)	–	–	109.9, 57.8, 53.5, 36.8 and 12.2	LIMs	PSO	–	[66]
FA-based Gpolymers	Cu(II)	6	180	40	LIMs	PSO	Endothermic	[67]
Magnesium oxide (MgO) incorporated FA composite (FAMgO)	RB5 azo dye	10	90	48.78	LIMs	PSO	Endothermic	[68]
Iron oxide/aluminum hydroxide composite loaded on coal FA (FA3)	Cr(VI)	6	480	33.3	FIMs	PFO	Endothermic	[69]
Swine manure	MB	7	–	143.76	LIMs	PSO	–	[70]
Rice straw biochars	MB	7	–	131.58	LIMs	PSO	–	[70]
Zeolite P1 from FA	NH_4	6	40	22.9	LIMs	PSO	Exothermic	[71]
Zeolite P synthesis based on FA	Cu(II)	–	–	138.1	LIMs	PSO saturation model (SESSM)	–	[72]
	Ni(II)			77.0		PFO empirical kinetic model (FEKM)		

Table 5 – Summarized details of some reported studies on FA-based adsorbents for removal of HMs and dyes.

Particle dimension (mm)	Surface area (m^2/g)	HMs/Dyes	pH	Dosage ($g.L^{-1}$)	Time of contact (hours)	Maximum adsorption capacity ($mg.g^{-1}$)	Removal effectiveness (%)	References
–	–	Pb^{2+}	6.0–7.5	6.0	1.50	–	˃80	[91]
0.200	–	Cu^{2+}	6.0	2.00	2.00	152.31	–	[62]
0.045	56.0	Cu^{2+}	6.2	1.50	72.00	98.40	–	[92]
0.071–0.090	–	Cu^{2+}	–	5.00	2.00	79.11	–	[93]
0.200	–	Pb^{2+}	5.0	1.40	2.00	174.34	–	[64].
0.030	–	Cu^{2+}	6.0	3.00	1.50	69.11	–	[56]
0.075	8.22	Cd^{2+}	5.0	0.08	7.00	26.25	–	[85]
–	56.00	MB/Crystal violet	6.3	0.2	–	38.38/97.92	85	[94]
0.045	25.70	MB/rhodamine B	˃9.0/˃6.0	1.0	–	17.00/1.90	90	[18]
0.09	28.50	Thionine (TH)/ safranine T (ST)	5.0–10.0	10.0	24.00	0.008/0.006	–	[83]
<0.20	–	MB	5.0	1.00	2.00	37.04	–	[95]
0.12–0.45	–	MB	11.1	2.00	–	0.669/0.696	89.15/92.79	[96]

constituents (faujasite FA and Gpolymer) was observed. The equilibrium values of the pH were reported to be greatly affected (increased compared to the original pH) by the adsorption effectiveness, possibly owing to the nature of alkaline lime (CaO) in these sorbent materials.

As reported by Xu et al. [80], Pb^{2+} sorption occurs at an equilibrium pH value of less than 6.0 (which is equivalent to the original pH value within 3.0) and was ascribed to the opposition between H_3O^+ and Pb^{2+} on the adsorbent locations' surface. At the original pH value of less than 3.0, all of the equilibrium values of the pH are greater than 7.0, but less than 7.8; indicating that the precipitation of Pb^{2+} is possibly insignificant under entire equilibrium circumstances. The amounts of the adsorption by faujasite and Gpolymer practically keep constant at 74.0 mg g^{-1}, due to fact that the Pb^{2+} positive ions in the solutions reduced the quantity of saturation. While the amount of the adsorption by FA to some extent rises when the original pH value was higher than 4.0.

Some other studies such as the one of [81], reported that the optimal pH values for adsorption Cd^{2+}, Pb^{2+} and Zn^{2+} by alkaline stimulated FA ranged from 5.5 to 6.6. Also [64], revealed that the original pH value under which the highest acceptance capacity for Pb^{2+} by FA-based Gpolymer was 5.0, but they were silent about the final pH value. While Wang et al. [82], reported that the pH value of Pb^{2+} positive ions started precipitation at 7.86 at an original concentration of 300.0 mg/L, which according to them is estimated from the precipitation constant of $Pb(OH)_2(s)$, 1.20×10^{15}.

The impact of pH on dye adsorption (DA) at some preliminary pH media under similar circumstances with kinetic experiments using FA-based adsorbent was studied by [83]; their results revealed that the DA of two (2) dyes on using FA-based adsorbent to some extent rises at lesser pH and a sharp increase was detected in pH value greater than 9.0. While the DA on the zeolitized FA products was to some extent subjected to the pH and approximately constant in the pH value ranging from 5.0 to 10.0.

The sorption elimination of an anthraquinone dye and an azo dye from single and binary solutions utilizing FA was comparatively reported by [35]. The percentage of removal of anthraquinone dye was reported to be 72.90% at a pH value of 2.25. But was strappingly reduced when the pH value was increased (ranging from 3.14 to 7.90) from 69.50% to 6.56%. According to Qiu et al. [43], the pH solution which is a critical parameter in the procedure of adsorption of HMs and dyes critically influence the capacity of the adsorption of the zeolites; in their study, the pH dependency experiment on the adsorption capacity was

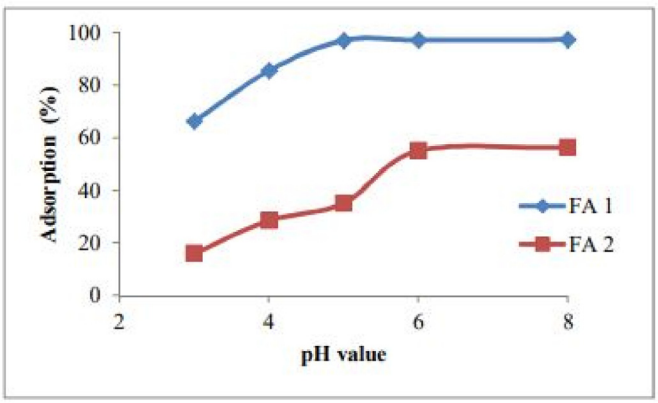

Fig. 10 – Effect of pH on the removal percentage (%) of Cu^{2+} ions [73].

understudied to determine its influence. In the result, it was shown that the elimination quantities for diverse ions raised with the preliminary pH value. At a pH value of 4.0, Cu^{2+} ions and Pb^{2+} ions were almost entirely detached, and all other ions (except the Mn^{2+} ions) were detached at a pH value of 6.0. Owing to the alkaline feature of FA, modified zeolite constituents displayed high pH adapt-capability to that of metal solutions.

The influence of pH on the adsorption of HMI by the produced zeolite at pH values ranging from 1.0 to 12.0 as reported by He et al. [74], is shown in Fig. 11. The study was carried out with a zeolite having a dosage of 5.0 g L^{-1} and an IConc value of 100.0 mg L^{-1}. The elimination effectiveness was reported to be lower than 10.0% for all the respective HMI used, at a pH value of 1.0, and it raised swiftly as the value of the pH raised from 1.0 to 5.0. Correspondingly, the elimination effectiveness for the various HMI was 63.0%, 80.0%, 93.0%, 98.0% and 99.0% for Mn^{2+}, Ni^{2+}, Cd^{2+}, Cu^{2+} and Pb^{2+}, at an original pH value of 5.0.

From several reported studies, it is observed that the solution of the pH has a noticeable consequence on the adsorption of HMs and dyes on several adsorbents. In a specific range of pH value, HMs and dyes adsorption upsurges with rising pH values up to a convinced value and then reduce with a further rise in the pH value. Hence, the consequence of pH could also be described in terms of the pH at the point of zero (nil) charge, at which the charge on the surface of the adsorbent is at nil charge [84,85]. Albeit, from Table 4, which contains a summary of some existing studies on the use of FA-based adsorbent and the respective contaminants, optimum pH values, the time of adsorption, the maximum sorption capacity, the thermodynamics and adsorption process, it was observed the pH on the adsorption process of HMs and dyes using FA-based adsorbent range from 3.0 to 8.0.

4.2. *Effect of adsorbent dosage*

The adsorbent dosage is also one of the significant parameters that influence the adsorption process of HMs and dyes using FA-based adsorbent because it controls the capacity of an adsorbent for a specified original concentration of the adsorbed constituents [73]. Adsorbent dosage is a critical procedure parameter for defining an adsorbent's potential for a given quantity of adsorbent under operating conditions [86]. The important parameters to consider are the amount of adsorbent and adsorbate used to impact the extent of HMI and DA [87].

Studies on intra-particle diffusion have shown that the dimension of the particles of the adsorbents significantly impacts the degree of adsorption particularly for HMs and dyes. Reduction in the size of the particles can result in an upsurge in the surface area and consequently a rise in the adsorption possibilities at the external surface of the adsorbents. Also, there is an opportunity for the diffusion of the intra-particle from the external surface into the pores of the substance. The capacity of adsorption of waste materials depends on the available specific surface area for the solute interaction of the surface. Expectedly, several studies have shown that the capacity of adsorption will rise with a greater surface area. Conversely, minor particle size upsurges the capacity of the adsorption [64,88–90].

Darmayanti et al. [73], reported the consequence of adsorbent dosage on the elimination of Cu^{2+} ions; it was observed from the results that the efficiency of the adsorption raised from 24.90 to 93.90% and from 29.30 to 56.70% as the dosage raised from 1.00 to 10.00 g L^{-1} for the first and second FA (used for the study) respectively. According to them, the upsurge is described by the rise in surface area and the accessible adsorption locations of the FA. With raising FA, the accessible locations for binding Cu^{2+} ions rise and thus improves the adsorption efficiency (Fig. 12).

Dogar et al. [33], investigated the influence of the adsorbent dosage on the elimination effectiveness of dyes by changing the quantities of functionalized biomass FA (ARS) and amine-functionalize biomass FA adsorbents (BTB) (5.0, 10.0, 15.0, 20.0, 25.0, and 30.0 mg), where some specific quantities of adsorbents were added to 10.0 mL dye media at room temperature with enhanced pH values of 4.0 and 5.0, and time of contact 10 min and 5 min respectively as illustrated in Fig. 13 (a and b). For both dyes, functionalize biomass FA displayed greater adsorption capacity as compared to the amine-functionalize biomass FA adsorbents. Table 5 contains summarized details of some reported studies on FA-based adsorbents for the removal of HMs and dyes.

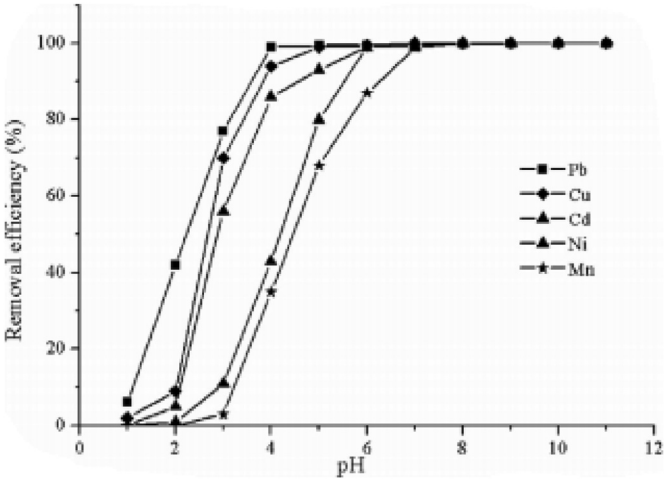

Fig. 11 – Effect of initial pH [74].

4.3. *Effect of initial concentration*

The IConc of HMs and dyes have a sturdy consequence on the adsorption capacities of several adsorbents specifically the FA-based adsorbents [97]. As reported by [73], the IConc of the adsorbent is also one of the significant parameters that influence the adsorption process of HMs and dyes using FA-based adsorbent since it controls the capacity of an adsorbent for a specified IConc of the adsorbed constituents. Generally, the adsorption capacity is proportional to the concentrations of the HMs and dyes (they increased as the concentrations increased) [98].

However, several studies have revealed that the removal effectiveness of HMs and dyes depend on the concentration and there is a declining tendency with an upsurge of the IConc. The consequence of time of contact and the IConc on the adsorption of Cu^{2+} on FA-based Gpolymer was reported by [62]. It was revealed from this study that increasing the contact time from 5 to 15 min meaningfully improved the rate of elimination of Cu^{2+}, and only a minor change in removal effectiveness took place from 15 to 180 min. The Cu^{2+} elimination effectiveness remained greater than 80% when the IConc was lower than 140.0 mg L^{-1}.

Also, the results of [92] indicate that the adsorption effectiveness of Cu^{2+} on Gpolymer was reported to be concentration-dependent; indicating that the greater the IConc, the smaller the removal effectiveness.

It was also reported by [64], that the adsorption of Pb^{2+} ions on Gpolymer raised with an upsurge in the time of contact and then attained the highest value after 120 min and remained unchanged. The elimination effectiveness remained at a very high level greater than 80.0%, with the IConc below 140.0 mg L^{-1}. With the low IConc, the obtainable pores in the surface of the adsorbent were enough to adsorb most of the HMs, which had occupied the likely existing locations so that the adsorption effectiveness rises to a certain extent. As the IConc rises, the available locations become insufficient to adsorb them, consequently, a main portion of the HMs remain in the solution.

Also [99], discovered that the adsorption procedure for granular solids was not that fast, where 24 h is needed to attain the time of equilibrium, however for samples that are pulverized, the time of equilibrium was attained at a time 30 min. They however recommended that substantial time is needed for the diffusion of HMI through the bulk of mesoporous Gpolymer and the means of adsorption was considered to be

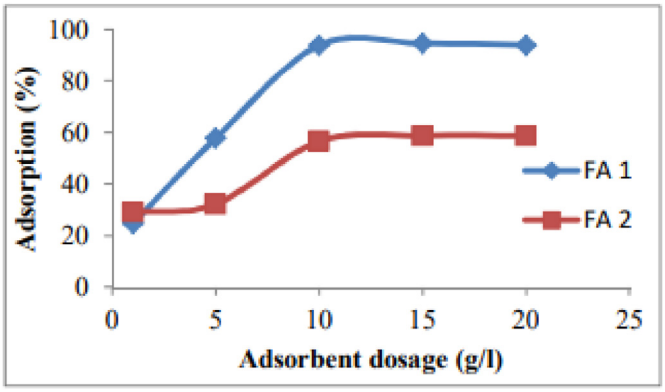

Fig. 12 – The consequence of adsorbent dosage on the elimination effectiveness (%) of Cu^{2+} ions [73].

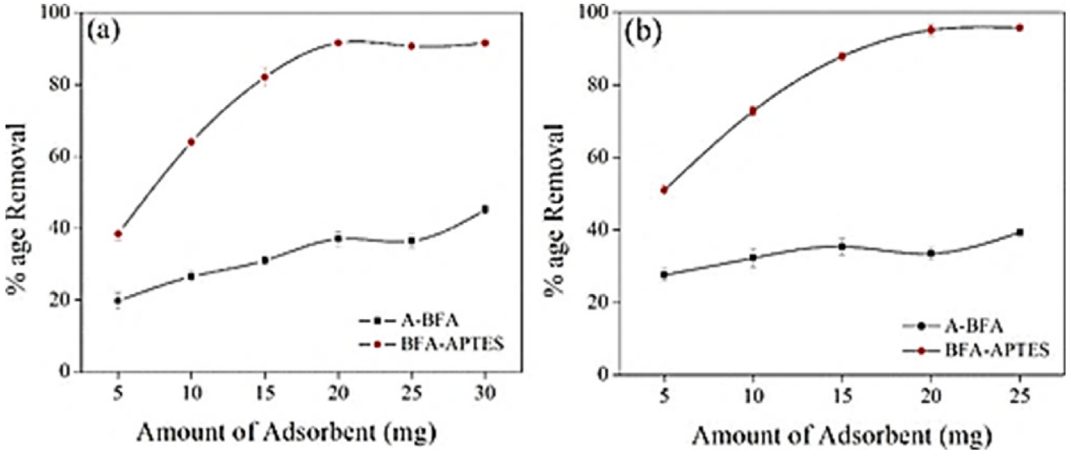

Fig. 13 – Effect of the amount of adsorbent (a) ARS and (b) BTB [33].

the exchange of ions and electrostatic adsorption of HMI on the negatively charged Al tetrahedral of the Gpolymer matrix.

4.4. *Effect of co-existing ions/ionic strength*

The co-existing ions/ionic strength (which is also known as the electrolyte concentration) of a solution affects the binding force of the adsorbate and adsorbent during the adsorption process of HMs and dyes using FA-based adsorbent or other adsorbents; it affects the potential and width of the interface of the dual-layer round the adsorbent [6].

According to Wen et al. [49], the coexisting ions in an aqueous medium was found to contend with HMI for the adsorption sites on adsorbents in this study. Hence in the study carried out by He et al. [74], the separate effects of coexisting positive ions of Al^{3+}, NH^{4+}, Ca^{2+}, Mg^{2+} and Na^{+}. that are habitually existing in aqueous media were examined with an IConc of 0.10 M. Also, the Blank experiment was carried out without coexisting positive ions; this was carried out at an IConc of 100.0 mg/L, dosage of zeolite of 10.0 g/L, and pH of 5.0, ad the results are shown in Fig. 14. From Fig. 14, it was shown that the removal effectiveness of HMs was reduced meaningfully with the existence of coexisting positive ions. The decrease inclination which evidently confirmed the consequence of the positive ions was reportedly in the order of "$Al^{3+} > NH^{4+} > Ca^{2+} > Mg^{2+} > Na^{+}$".

Umejuru et al. [100], investigated the influence of co-existing ions on some HMI using the IConc of 50.0 mg/L from on Cd^{2+} ions as well as diverse concentrations (20.0, 30.0, 50.0, and 100.0 mg L^{-1}) from Cu^{2+} and Pb^{2}, with an adsorbent dosage of 0.40 g, a sample volume of 50.0 mL and time of contact of 24 h using coal FA coated with carbon hybrid NMs. It was observed for the results that some positive ions (on Cu^{2+} and Pb^{2+} ions) might exit with Cd^{2+} in wastewater and water natural. Hence, they suggested that it is essential to selectively eliminate the targeted HMI only. Consequently, the study affirmed the selectivity of Cd^{2+} between diverse HMs using carbon hybrid NMs (Fig. 15); where the adsorption of Cd^{2+} onto carbon hybrid NMs was reported not affected by other HMs, hence showing that carbon hybrid NMs is highly selective to the removal Cd^{2+} ions.

5. Mechanism of adsorption using isotherms, kinetics and thermodynamics

5.1. *Adsorption isotherm*

The adsorption isotherms and kinetics are regularly used to examine the process of adsorption, mechanism and performance. Imperatively, isotherms provide information about adsorption systems, adsorption process, surface properties of the adsorbents and draws a relationship between adsorbates and adsorbents. To explore the most fundamental sorption mechanisms, numerous characterization approaches coupled with theoretical calculations which are supported with powerful theoretical models are invoked. Tables 6 and 7 enumerates some of these models [11,40,69].

Based on the reviewed publications in this work, (see Table 6), it is apparent that FIMs and LIMs are the most often employed isotherms. FIMs assumes multilayer adsorption on a different surface whereas LIMs is built on the presumption that sorption happens evenly on the active sites of the sorbent and that the sorption process becomes complete at these sites when all the sites are fully filled by sorbates. The linearized form of FIMs is given in Eq. (3) [11,40,69]:

$$\log Q_e = \log K_F + \frac{1}{n}\log C_e \tag{3}$$

where Q_e ($mg.g^{-1}$) and C_e ($mg.L^{-1}$) respectively represent the equilibrium adsorption capacity of adsorbent and the equilibrium concentration of adsorbate. The n and K_F ($mg.g^{-1}$) $(mg.L^{-1})^n$ are FIMs constants associated with intensity and adsorption capacity respectively. The constants are obtained from the slope and intercept of a linear–line graph of log Q_e vs log C_e. The *n* specifies the magnitude of the adsorption driving force or the surface heterogeneity. Particularly, when $1/n > 1$, co-adsorption ensues while a normal L-type is epitomized when $1/n < 1$ [11,40,69].

Eq. (4) epitomizes a linear form for LIMs. The parameters Q_e ($mg.L^{-1}$), Qm ($mg.g^{-1}$), Ce and K_L are the equilibrium adsorption capacity, the maximum adsorption capacity, the equilibrium concentration of adsorbate and is the constant linked

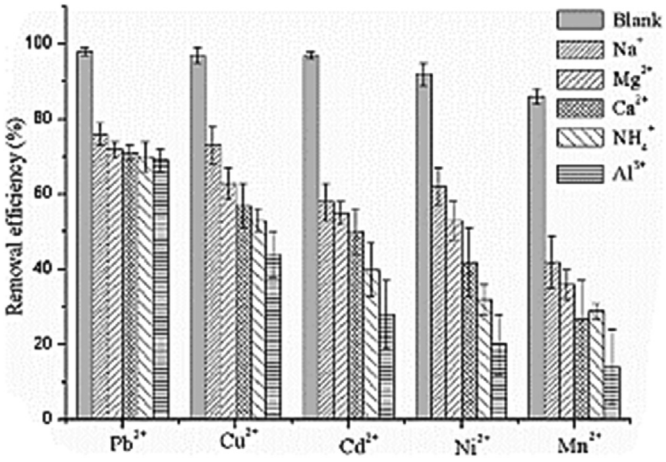

Fig. 14 – The consequence of coexisting ions on the removal effectiveness of HMI [74].

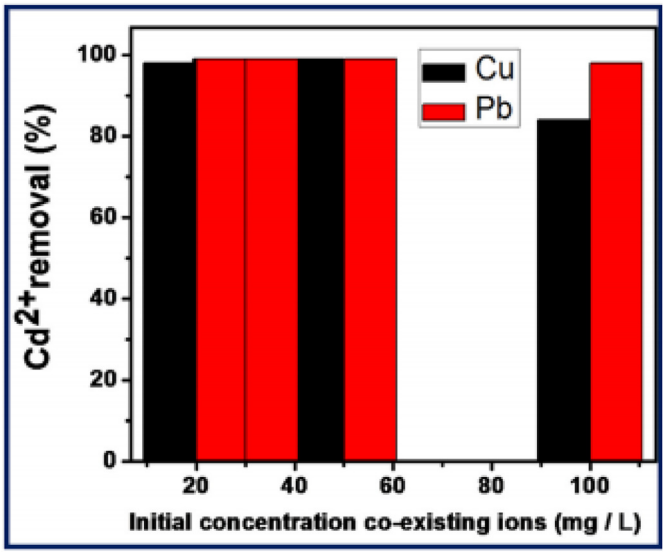

Fig. 15 – Effect of co-existing ions [100].

Table 6 – Isotherm models [11,69].

Isotherm model	Equation
FIMs	$Q_e = K_F C_e^{1/n}$
LIMs	$Q_e = \frac{Q_m K_L C_e}{1 + K_L C_e}$
Redlich–Peterson	$Q_e = \frac{K_R C_e}{1 + \alpha_R C_e^{\beta}}$
Temkin	$Q_e = \frac{RT}{b} \ln K_T + \frac{RT}{b} \ln C_e$
Henry	$Q_e = K_H C_e$
Dubinin–Radushkevich	$Q_e = Q_m e^{-k\varepsilon^2}$
Sips	$Q_e = \frac{Q_m \alpha_s C_e^{1/n}}{1 + \alpha_R C_e^{\beta}}$

Table 7 – Kinetic models [11,40,69].

Kinetic model	Equation
Pseudo-first order	$Q_t = Q_e(1 - e^{-k_1 t})$
Pseudo-second order	$Q_t = \frac{k_2 Q_e^2 t}{1 + k_2 Q_e t}$
Elovich	$Q_t = \frac{1}{\beta} \ln(\alpha\beta) + \frac{1}{\beta} \ln t$
Bangham	$\ln Q_t = \ln k_b + \frac{1}{m} \ln t$

to the adsorption energy. The viability of adsorption is anchored on the R_L (known as separation factor) expressed in Eq. (5) [11,40,69].

$$\frac{C_e}{Q_e} = \frac{C_e}{Q_m} + \frac{1}{K_L Q_m} \tag{4}$$

$$R_L = \frac{1}{1 + K_L C_0} \tag{5}$$

where C_0 is the IConc capacity. The dimensionless separation factor R_L has the following four key inferences. When $0 < R_L < 1$, represents a favorable isotherm implying successful interaction between adsorbate and adsorbent; when $R_L = 0$ it embodies an irreversible isotherm; $R_L > 1$, depicts unfavourable isotherm; and finally, when $R_L = 1$ it shows a linear isotherm [11,40,69].

These two models together with others (Table 6) have been used widely to explore, examine and elucidate data obtained using FA related sorbents. For instance, raw FA and modified FA (MFA) was employed for the removal of HMI (Zn^{2+}, $Pb^{2+}$and As(V)) [69]. It was recognized that some factors such as the co-existence of physisorption, heavily soluble salts, surface interactions, and chemosorption and electrostatic interactions affect the removal of target compounds. LIMs, FIMs, Temkin and Dubinin–Radushkevich isotherms were used in this study. LIMs was found to best described the procedure and the model was adopted to calculate the adsorption capacity. The maximum adsorption capacities for Pb^{2+}, As(V) and Zn^{2+} was discovered to be 26.06, 29.71 and 33.13 mg g^{-1} respectively.

Attari et al., [40] produced zeolite Linde Type A (LTA) from coal FA (CFA-ZA) for the removal of mercury from industrial water. With 10.0 mg/L IConc, a remarkable 94.00% mean removal efficiency of the CFA-ZA for Hg(II) was witnessed which compares well with activated carbon. Temkin, LIMs and FIMs were utilized for the study. Based on the R^2 values, to some extent, the three models explained the adsorption of Hg(II) on the CFA-ZA. Outstandingly, the FIMs was superior since it offers assumptions of physical adsorption on heterogeneous (diverse) surfaces exhibiting heterogeneous (diverse) energy distribution and it elucidates reversible (alterable) adsorption which is not constrained to the creation of a single-layer (monolayer).

Castillo et al. [23], using a silicate extract as precursor from FA, synthesized mesoporous silica (with a surface area of 282.00 m^2 g^{-1} and pore size of 5.70 nm) like mesoporous hexagonal silica (HMS) and functionalized it with ethylene diamino moieties through SAMMs method as an adsorbent for

sulfate in water. A remarkable adsorption time of 5 min with an optimum pH of 8.0 was observed. LIMs and FIMs studies revealed that the FIMs best explained the procedure with the highest adsorption capacity of sulfate being 146.10 mg g^{-1}.

A study based on the design and fabrication of Gpolymer aimed to be used as efficient HMI removal is reported by [67]. A structural alteration of FA using K^+ and Na^+ showed that Na^+-based alkali exhibited a more organized structure when compared to K^+-based alkali. The Gpolymer formed showed a more improved Cu^{2+}adsorption capacity of 40.00 mg/h when compared to the FA sample whose adsorption capacity was found to be 7.00 mg g^{-1}. LIMs, FIMs and Temkin isotherm models studies revealed that the adsorption was well described by LIMs. This can be attested from Table 6, that FIMs and LIMs were the mainly used isotherm models that best described the confiscation of several HMI and dyes onto FA sorbents thus implying monolayer and multilayer types of sorptions.

5.2. *Kinetics studies*

Adsorption kinematics studies provide information regarding sorbate diffusion processes, adsorption rates and rate-limiting steps [42,48]. They aid in setting experimental conditions and ensuring attainment of the equilibrium within a practical time. In batch sorption processes, several models like PFO, PSO, intraparticle, Elovich etc. have been used to explain the dispersion of solutes at the sorbent surface and in the pores.

As shown in Table 7, the PFO and PSO are the predominant kinetic models that best describe sorption data presented in this work and they can be represented linearly by Eqs. (6) and (7) respectively. PFO model is built on the postulation that the rate of variation of adsorbed solute with time is proportionate to the change in the equilibrium adsorption capacity and adsorbed quantity, while the PSO model assumes that the rate-limiting phase involves chemisorption relating to the valency forces via the exchange of electrons or sharing of electrons between sorbate and sorbent [55,69].

$$\log(Q_e - Q_t) = \log(Q_e) - \left(\frac{K_1}{2.303}\right)t \tag{6}$$

$$\frac{t}{Q_t} = \frac{1}{k_2 Q_e^2} + \left(\frac{1}{Q_e}\right)t \tag{7}$$

where Q_t and Q_e are adsorption capacities at time t and equilibrium time respectively; k_1 and k_2 constants for PFO rate and PSO rate respectively.

The intraparticle diffusion model (Eq. (8)) is precisely employed to describe the diffusion means of the adsorption procedure.

$$q_t = K_{id}(t)^{0.5} + C \tag{8}$$

where K_{id} (mg $g^{-1}h^{-0.5}$) stands for intraparticle diffusion rate constant while C is the intercept. The C has a characteristic relationship with the boundary layer thus the higher the value of C, the larger the effect of the boundary layer ensues. To attest that the adsorption mechanism obeys this model, a linear relationship is obtained when q_t versus $t^{1/2}$ is plotted and the values K_{id} and C can be found through linear fitting analysis [55].

The Elovich model (Eq. (9)) was first recognized to describe gas adsorption on solid sorbents. However, lately, it has effectively been employed to explain the adsorption of varied constituents from aqueous solutions on solids.

$$\frac{dq_t}{dt} = \alpha e^{-\beta q_t} \tag{9}$$

By using boundary conditions $q_t = 0$ and $t = 0$, in the integrations of Eq. (8) and with an assumption that $\alpha.\beta.t \gg 1$, leads to Eq. (10).

$$q_t = \beta \ln(\alpha\beta) + \beta \ln(t) \tag{10}$$

The model explains activated adsorption and presumes an energetically heterogeneous solid surface of sorbent meaning interaction between adsorbed particles does not affect the kinetics of adsorption [40]. For instance, three models namely PFO, PSO and intraparticle have been used during the kinetic studies in the treatment of Cr(VI) from aqueous solution using zeolite (ZFA) prepared using the raw FA (RFA). The study established that optimum operating conditions of pH (2.0), IConc of (50.00 mg L^{-1}) and adsorbent dosage (0.20 g) was ideal. Sorption kinetics by PFO, PSO and intraparticle diffusion models revealed that the process was fast and overall, the procedure was well defined by the PSO model [55].

Likewise, sorption studies of ammonium from Bleached Kraft Mill Effluents (BKME) on sepiolite and FA are reported [48]. It was established that below a pH of 5 and above the pH of 8, ammonium removal decreased. Equally, a decrease in particle sizes of FA and sepiolite resulted in an increase in adsorption with equilibrium attained after nearly one hour for both adsorbents. Three kinetic models namely; PFO, PSO and intraparticle were used. Intra-particle revealed that the sorption process exhibits two separate stages; external diffusion and diffusion of inter-particle. For both adsorbents, the PSO was found to describe the process well with ($r^2 \geq 0.99$) compared to the PFO model ($r^2 \leq 0.90$).

A comparative study to evaluate the efficiencies of three adsorbents; FA, FA-based Gpolymer and faujasite block for sorption of Pb from aqueous solutions. At the pH of 3.0, the adsorption capacities for faujasite, Gpolymer and FA was found to be 49.80, 118.60, 143.30 mg g^{-1} respectively. The process attained maximum adsorption equilibrium for 150 min for Gpolymer and faujasite while for raw FA the process attained a maximum of 240 min. Equally, the kinetic studies revealed that the PSO model fitted well for faujasite and Gpolymer whereas PFO described the kinetic process for FA. The findings fronted Gpolymer as an energy-saving, environmentally friendly and low-cost adsorbent with similar adsorption mechanisms to zeolite materials and faujasite [42].

Also, Asl et al. [69], produced a hydrous iron oxide/aluminum hydroxide compound fused on coal FA for the elimination of Cr (VI) from an aqueous solution. The study recorded the highest percentage removal of 84.90% and 33.30 mg g^{-1} as maximum sorption capacity during a contact time of 8 h, adsorbent dose of 2.0 g L^{-1} and optimum pH of 6.0 and IConc of 53 mg/L kinetics studies using intra-particle, PFO and PSO models were done with the analysis revealing that the process was controlled by PFO. The statistical analysis coupled

with experimental data effectively exhibited that the synthesized sorbent was efficient in Cr(VI) removal from wastewater.

5.3. *Thermodynamic studies*

Temperature plays a fundamental role in the sorption process given that an increase in sorption capacity corresponds to a rise in temperature. Equally, it influences the amount of diffusion of HMI in solution, mobility and proportion, sorbent active sites as well as transforming chemical interface [11]. Therefore, in the assessment of the effect of temperature, thermodynamic parameters ought to be determined for practical applications. The enthalpy, free energy and entropy are specifically used to examine the spontaneity of the sorption procedures and these parameters can be deduced from Eqs. (11) and (12) [69].

$$\ln K_c = \left(\frac{\Delta S}{R}\right) - \left(\frac{\Delta H}{RT}\right) \tag{11}$$

$$\Delta G = -RT \ln K_c \tag{12}$$

where Kc is the thermodynamic equilibrium constant, ΔS is entropy change ($J.mol^{-1}$), ΔH is the enthalpy change ($J.mol^{-1}$), ΔG is the Gibbs free energy, R is the universal gas constant (8.314 J/mol K) and K is the temperature.

In the studies carried out by [69], was centered on the sorption of Cr(VI) onto FA3 at various temperatures (25, 35 and 45 °C). It was realized that the enthalpy change (ΔH) was positive showing that the sorption process of Cr (VI) onto FA3 was endothermic. Also, randomness at the solid–liquid interface was affirmed by ΔS having a positive value. The decrease in value at a higher temperature of ΔG and its negative values indicated feasibility and spontaneity sorption of Cr(VI).

Moreover, Zeolite P1 obtained from fluidized bed fly ash (FA) through a process of solvent-free was used in the removal of ammonium from water [71]. At temperatures of 298, 308 and 318 K, the determined thermodynamic ΔG values were −2.60, −2.37 and −1.99 kJ/mol respectively. These negative values depict that NH_4^+ adsorption by zeolite P1 is spontaneous and an increased of ΔG with intensification in the temperature reveals that the process is unfavourable at elevated temperatures. Likewise, ΔH and ΔS values of −11.61 kJ/mol and −0.030 kJ/(L.mol) correspondingly, showed that the adsorption of NH_4^+ on zeolite was exothermic and randomness decreased with NH_4^+ removal.

The influence of temperature on the sorption of tannic acid onto chitosan/NaOH/FA composite was examined [53]. The negative values of ΔG obtained here indicated a spontaneous and favourable adsorption process of tannic onto chitosan/NaOH/FA composite. Conversely, these values did not follow in the range of either physisorption (8.00 kJ/mol) or chemisorption (between 20.00 and 40.00 kJ/mol) showing that the adsorption process includes electrostatic attraction and ion exchange. The ΔH value was negative showing an exothermic adsorption process. Equally, from different isotherm constants, the ΔH values were 7.87–15.98 kJ/mol indicating in addition to electrostatic attraction, hydrogen bonding and organic partitioning are essential to the adsorption procedure. The study affirmed that the process of adsorption through ΔSexhibits an increase in randomness at an interface of the solid/liquid.

6. Regeneration and desorption studies

Regeneration and desorption studies aid in evaluating the retrieval and reusability of metal-encumbered adsorbent thus providing valuable information that may help in protecting the environment and minimizing operational cost. Extensive research studies on desorption and regeneration have been performed using FA-based adsorbent and remarkable results reported. For example, fired coal FA desorption studies have been conducted to approximate the metal realizing capacity of pellets encumbered with Cu and Cd [101]. The saturated Cu and Cd pellets were dehydrated at 60.00 °C and then 5.00 g added into a glass reactor comprising 200.00 mL of an aqueous solution whose persistent temperature was 25.00 °C. Subsequently, the ensued pulp was stirred at 140.00 rpm and some samples were inhibited at various time intervals and using atomic adsorption spectrophotometry, metal content was analyzed. Four different solutions were employed to carry out desorption experiments; two acidic solutions arranged from acetic acid having pH values of 2.88 ± 0.05 and 4.98 ± 0.05 and the other two solutions arranged from pure deionized water (neutral solution) and an alkaline solution of NaOH with a pH value of 12.0. The experimental results revealed that no Cu and Cd desorption in the neutral and alkaline solutions after an equilibrium time of 72 h. This was attributed to the high adsorption affinity of Cu and Cd at these conditions which makes the surface metal complexes extremely stable. Conversely, in acidic solutions, high quantities of Cu and Cd were desorbed and the process intensified in this region since Cu and Cd have a small affinity at these conditions. Generally, the results showed that Cu was desorbed to a higher degree in comparison to Cd under similar experimental circumstances.

Similarly, coal-fired FA (CFFA) desorption studies of Cd (II), Cu (II) and Ni (II) have been conducted to evaluate cost-efficiency [102]. The experiments were executed using 0.10 M of HCl, H_2SO_4 and HNO_3 as stripping agents with the metal-laden adsorbed in a flask being stirred at 150.00 rpm for 24 h. Through this process, filtrates were evaluated and the desorbed heavy metal ion percentage evaluated. Successive bio-sorption-desorption cycles were then repeated three times (cycles) for similar adsorbents. During these cycles, an observation of loss in weight was witnessed. During the initial two cycles, a substantial weight loss was noticed, due to the washing of soluble substances while the final cycle had no substantial loss of weight. It was concluded that the steady decay in the sorption process with an upsurge in the number of cycles was a result of the corrosive nature of the acid and washing out of the existing functional group at the surface of the sorbent. Desorption results showed maximum values with 0.1 N H_2SO_4 which followed with a percentage of 79.8, 72.1, and 67.3 for Cu, Ni and Cd respectively. Likewise, a declining trend followed $H_2SO_4 > HNO_3. > HCl$.

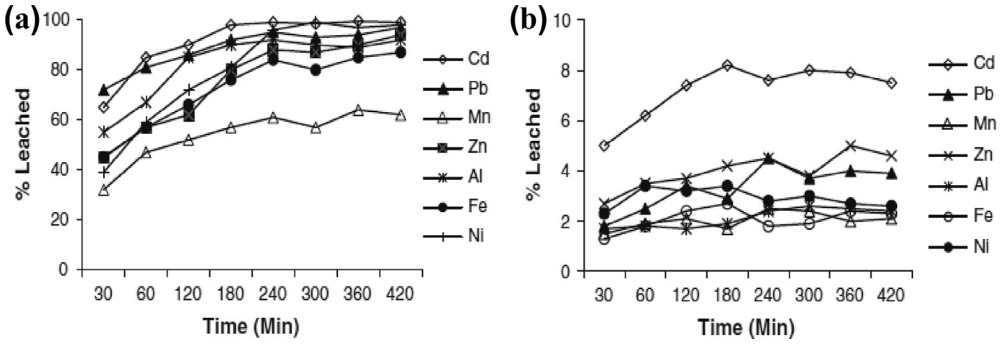

Fig. 16 – Desorption studies for various HM (a) acidic media and (b) neutral media [47].

Sahoo et al. [47], using modified FA adsorbent obtained from coal FA and modified through alkali hydrothermal treatment carried out Cd, Pb, Mn, Zn, Al, Fe and Ni desorption studies. These studies were conducted both in acidic and neutral solution using metal-laden MFA improved during adsorption experiments. The acidic solution of pH of 2.0 and neutral solution of pH 6.5 was used. The recovered 30.0 g of MFA was treated in 1.0 L solution, shaken at various intervals of time for 7 h then collected, filtered and analyzed. The desorption results (Fig. 16) showed that in the acidic media the desorption was significant compared to the neutral media. At the initial 3 h, except Mn with 57.00%, other metals were desorbed over 76.00–98.00% then slow rates followed afterwards. Equally, in the neutral media, with an exception of Cd with 8.20% while the remaining metals had low amounts of less than 5.00%. This desorption study indicates that metal confiscated in FA remains steady over time a fact attested by a small percentage of adsorbed metal realized. The maximum recovery of HMs from MFA made in the acidic solutions can be attributed to FA becoming protonated and failure to attract the positively charged HMI hence the protons substitute the bound ions.

From the reviewed desorption studies, it is apparent that most HMI was significantly desorbed in the acidic solutions inferring that the FA-based adsorbents could be efficiently regenerated, renewed and further re-used.

7. Conclusion

Owing to the unique and distinctive properties of FA-based adsorbents or modified FA such as their suitable pore dimension, alkalinity, negative charge, unburned carbon residual, exceptional permeability and surface area as well as their cost-effective and eco-friendly tendencies, they are presently used for the removal of HMs and dyes from AMD and acidic industrial effluents, by defusing the pH to eliminate the HMs and dyes. The removal of HMs and dyes was reported conceivably due to the adsorption and precipitation on the surface of the adsorbents. Based on the reviewed publications, LIMs and FIMs best described the sorption process thus signalling monolayer and multi-layer sorptions. PSO provided the best fit in elucidating the kinetic process and both exothermic and endothermic processes revealed the nature of the thermodynamic process during sorption. It is however suggested that further research on the utilization of FA-based adsorbent for the elimination of HMs and dyes from wastewater, should concentrate on advancing and evolving the limitations in previous studies as well as the use of FA-based Gpolymer particles since it has been reported by some studies that the magnetic FA-based Gpolymer could more effectively in neutralizing pH and removing HMs and dyes from industrial acidic effluent or domestic water arrangements. Hence, the magnetic Gpolymer could be utilized as a useful tool, where the removal of HMs and dyes are needed to be trailed by separation of the adsorbents with the prospect of recovery of HMs and dyes and recycling of the adsorbents.

To advance the capacity of adsorption and effectiveness of FA on the removal of HMs, dyes and other environmental contaminants, and gain full benefits of FA, innovative technologies for the effective utilization of FA should be evolved and advanced, such as the nanofibre technology. In utilizing such recent nanotechnological mechanisms, FA can be further synthesized into affordable, multi-efficient and multipurpose absorbent hybrid composites for the adsorption of both atmospheric, aquatic and terrestrial environmental contaminants; hence, FA absorbent hybrid composites are evolving material that has a great future prospect. Consequently, since it is inferred from existing literatures that the FA-based adsorbents for HMs and dyes can be proficiently regenerated and further re-used, it is therefore suggested that further studies and advancement in this regard should be encouraged and strengthened.

Funding

This research work has not in any way benefited from research funding or grants from any commercial, agencies or non-profit organizations.

Declaration of Competing Interest

The authors declare that they have no known competing financial interests or personal relationships that could have appeared to influence the work reported in this paper.

Acknowledgements

The authors are appreciative to their different institutions and authors whose publications were utilized for this review study.

REFERENCES

[1] Anjum M, Miandad R, Waqas M, Gehany F, Barakat M. Remediation of wastewater using various nano-materials. Arab J Chem 2019;12(8):4897–919.
[2] Olivera S, Muralidhara H, Venkatesh K, Guna V, Gopalakrishna K, Kumar Y. Potential applications of cellulose and chitosan nanoparticles/composites in wastewater treatment: a review. Carbohydr Polym 2016;153:600–18.
[3] Jawed A, Saxena V, Pandey L. Engineered nanomaterials and their surface functionalization for the removal of heavy metals: a review. J Water Proc Eng 2020;33:101009.
[4] Yu G, Lu Y, Guo J, Patel M, Bafana A, Wang X, et al. Carbon nanotubes, graphene, and their derivatives for heavy metal removal. Adv Compos Hybrid Mater 2018;1(1):56–78.
[5] Duan C, Ma T, Wang J, Zhou Y. Removal of heavy metals from aqueous solution using carbon-based adsorbents: a review. J Water Process Eng 2020;37:101339.
[6] Ali M, Hoque M, Safdar Hossain S, Biswas M. Nanoadsorbents for wastewater treatment: next generation biotechnological solution. Int J Environ Sci Technol 2020;17:4095–132.
[7] Singh S, Barick K, Bahadur D. Functional oxide nanomaterials and nanocomposites for the removal of heavy metals and dyes. Nanomater Nanotechnol 2013;3:3–20.
[8] Naseem T, Durrani T. The role of some important metal oxide nanoparticles for wastewater and antibacterial applications: a review. Environ Chem Ecotoxicol 2021;3:59–75.
[9] Aigbe U, Osibote O. A review of hexavalent chromium removal from aqueous solutions by sorption technique using nanomaterials. J Environ Chem Eng 2020:104503.
[10] Aigbe U, Ho W, Maity A, Khenfouch M, Srinivasu V. Removal of hexavalent chromium from wastewater using PPy/Fe3O4 magnetic nanocomposite influenced by rotating magnetic field from two pole three-phase induction motor. J Phys: Conf Ser 2018;984:012008.
[11] Ukhurebor K, Aigbe U, Onyancha R, Nwankwo W, Osibote O, Paumo H, et al. Effect of hexavalent chromium on the environment and removal techniques: a review. J Environ Manag 2021;280.
[12] Aigbe U, Onyancha R, Ukhurebor K, Obodo K. Removal of fluoride ions using a polypyrrole magnetic nanocomposite influenced by a rotating magnetic field. RSC Adv 2020;10(1):595–609.
[13] Khairnar M, Jain V, Wadgave U, Dhole R, Patil S, Chopade S. Effect of different reverse osmosis water filters on fluoride content of drinking water. J Ind Assoc Public Health Dent 2018;16(2):165.
[14] Mekonen A, Kumar P, Kumar A. Integrated biological and physiochemical treatment process for nitrate and fluoride removal. Water Res 2001;35(13):3127–36.
[15] Carvalho F, Fucio S, Pascon F, Kantovitz K, Correr-Sobrinho L, Puppin-Rontani R. Effect of gamma irradiation on fluoride release and antibacterial activity of resin dental materials. Braz Dent J 2009;20(2):122–6.
[16] Li X, Wu X, Liu S, Li Y, Fan J, Lv K. Effects of fluorine on photocatalysis. Chin J Catal 2020;41(10):1451–67.
[17] Visa M, Chelaru A. Hydrothermally modified fly ash for heavy metals and dyes removal in advanced wastewater treatment. Appl Surf Sci 2014;303:14–22.
[18] Wang S, Boyjoo Y, Choueib A. A comparative study of dye removal using fly ash treated by different methods. Chemosphere 2005;60(10):1401–7.
[19] Onyancha R, Aigbe U, Ukhurebor K, Muchiri P. Facile synthesis and applications of carbon nanotubes in heavy-metal remediation and biomedical fields: a comprehensive review. J Mol Struct 2021;1238(130462):1–25.
[20] Bhateria R, Singh R. A review on nanotechnological application of magnetic iron oxides for heavy metal removal. J Water Proc Eng 2019;31:100845.
[21] Labied R, Benturki O, Eddine Hamitouche A, Donnot A. Adsorption of hexavalent chromium by activated carbon obtained from a waste lignocellulosic material (Ziziphus jujuba cores): kinetic, equilibrium, and thermodynamic study. Adsorpt Sci Technol 2018;36(3–4):1066–99.
[22] Lee S, Eom Y, Park J, Lee J, Kim S. Micro-hydrogel particles consisting of hyperbranched polyamidoamine for the removal of heavy metal ions from water. Sci Rep 2017;7(1):1–9.
[23] Castillo X, Pizarro J, Ortiz C, Cid H, Flores M, De Canck E, et al. A cheap mesoporous silica from fly ash as an outstanding adsorbent for sulfate in water. Microporous Mesoporous Mater 2018;272:184–92.
[24] Fiyadh S, AlSaadi M, Jaafar W, AlOmar M, Fayaed S, Mohd N, et al. Review on heavy metal adsorption processes by carbon nanotubes. J Clean Prod 2019;230:783–93.
[25] Kejriwal R, Mandke M, Ingle P. Bio-sorption of heavy metals: a review. Int J Adv Res Comput Sci 2018;5(11):32–42.
[26] Elumalai V, Brindha K, Lakshmanan E. Human exposure risk assessment due to heavy metals in groundwater by pollution index and multivariate statistical methods: a case study from South Africa. Water 2017;9(4).
[27] Asuquo E, Martin A. Sorption of cadmium (II) ion from aqueous solution onto sweet potato (Ipomoea batatas L.) peel adsorbent: characterisation, kinetic and isotherm studies. J Environ Chem Eng 2016;4(4):4207–28.
[28] Baby R, Saifullah B, Hussein M. Carbon nanomaterials for the treatment of heavy metal-contaminated water and environmental remediation. Nanoscale Res Lett 2019;14(1):1–17.
[29] Chubaka C, Whiley H, Edwards J, Ross K. Lead, zinc, copper, and cadmium content of water from south Australian rainwater tanks. Int J Environ Res Publ Health 2018;15(7). 2018.
[30] Visa M, Andronic L, Duta A. Fly ash-TiO_2 nanocomposite material for multi-pollutants wastewater treatment. J Environ Manag 2015;150:336–43.
[31] Zhang J, Ma C, Li H, Wang X, Ning F, Kang M, et al. Polyethyleneimine Modified Magnetic Microcrystalline cellulose for effective removal of congo red: adsorption properties and mechanisms. Fibers Polym 2021:1–14.
[32] Wekoye J, Wanyonyi W, Wangila P, Tonui M. Kinetic and equilibrium studies of congo red dye adsorption on cabbage waste powder. Environ Chem Ecotoxicol 2020;2:24–31.
[33] Dogar S, Nayab S, Farooq M, Said A, Kamran R, Duran H, et al. Utilization of biomass fly ash for improving quality of organic dye-contaminated water. ACS Omega 2020;5(26):15850–64.
[34] Wang S, Soudi M, Li L, Zhu Z. Coal ash conversion into effective adsorbents for removal of heavy metals and dyes from wastewater. J Hazard Mater 2006;133(1–3):243–51.
[35] Atun G, Ayar N, Kurtoğlu A, Ortaboy S. A comparison of sorptive removal of anthraquinone and azo dyes using fly

ash from single and binary solutions. J Hazard Mater 2019;371:94–107.
[36] Gadore V, Ahmaruzzaman M. Tailored fly ash materials: a recent progress of their properties and applications for remediation of organic and inorganic contaminants from water. J Water Proc Eng 2021;1:101910.
[37] Surabhi S. Fly ash in India: generation vis-à-vis utilization and Global perspective. Int J Appl Chem 2017;13(1):29–52.
[38] Gollakota A, Volli V, Shu C. Progressive utilisation prospects of coal fly ash: a review. Sci Total Environ 2019;672:951–89.
[39] Koshy N, Singh D. Fly ash zeolites for water treatment applications. J Environ Chem Eng 2016;4(2):1460–72.
[40] Attari M, Bukhari S, Kazemian H, Rohani S. A low-cost adsorbent from coal fly ash for mercury removal from industrial wastewater. J Environ Chem Eng 2017;5(1):391–9.
[41] Abd Malek N, Jawad A, Abdulhameed A, Ismail K, Hameed B. New magnetic Schiff's base-chitosan-glyoxal/fly ash/Fe_3O_4 biocomposite for the removal of anionic azo dye: an optimized process. Int J Biol Macromol 2020;146:530–9.
[42] Liu Y, Yan C, Zhang Z, Wang H, Zhou S, Zhou W. A comparative study on fly ash, geopolymer and faujasite block for Pb removal from aqueous solution. Fuel 2016;185:181–9.
[43] Qiu Q, Jiang X, Lv G, Chen Z, Lu S, Ni M, et al. Adsorption of heavy metal ions using zeolite materials of municipal solid waste incineration fly ash modified by microwave-assisted hydrothermal treatment. Powder Technol 2018;335:156–63.
[44] Li G, Wang B, Sun Q, Xu W, Han Y. Adsorption of lead ion on amino-functionalized fly-ash-based SBA-15 mesoporous molecular sieves prepared via two-step hydrothermal method. Microporous Mesoporous Mater 2017;252:105–15.
[45] Nguyen T, Tran T, Dao V, Vu Q, Nguyen T, Thai H. Using modified fly ash for removal of heavy metal ions from aqueous solution. J Chem 2020;9:1–11.
[46] Jiang X, Fan W, Li C, Wang Y, Bai J, Yang H, et al. Removal of Cr (VI) from wastewater by a two-step method of oxalic acid reduction-modified fly ash adsorption. RSC Adv 2019;9(58):33949–56.
[47] Sahoo P, Tripathy S, Panigrahi M, Equeenuddin S. Evaluation of the use of an alkali modified fly ash as a potential adsorbent for the removal of metals from acid mine drainage. Appl Water Sci 2013;3(3):567–76.
[48] Uğurlu M, Karaoğlu M. Adsorption of ammonium from an aqueous solution by fly ash and sepiolite: isotherm, kinetic and thermodynamic analysis. Microporous Mesoporous Mater 2011;139(1–3):173–8.
[49] Wen Y, Tang Z, Chen Y, Gu Y. Adsorption of Cr (VI) from aqueous solutions using chitosan-coated fly ash composite as biosorbent. Chem Eng J 2011;175:110–6.
[50] Chunfeng W, Jiansheng L, Lianjun W, Xiuyun S, Huang J. Adsorption of dye from wastewater by zeolites synthesized from fly ash: kinetic and equilibrium studies. Chin J Chem Eng 2009;17(3):513–21.
[51] Li F, Wu W, Li R, Fu X. Adsorption of phosphate by acid-modified fly ash and palygorskite in aqueous solution: experimental and modeling. Appl Clay Sci 2016;132:343–52.
[52] Wu X, Ma H, Zhang L, Wang F. Adsorption properties and mechanism of mesoporous adsorbents prepared with fly ash for removal of Cu (II) in aqueous solution. Appl Surf Sci 2012;261:902–7.
[53] Agarwal S, Rajoria P, Rani A. Adsorption of tannic acid from aqueous solution onto chitosan/NaOH/fly ash composites: equilibrium, kinetics, thermodynamics and modeling. J Environ Chem Eng 2018;6(1):1486–99.
[54] Chatterjee A, Basu J, Jana A. Alumina-silica nano-sorbent from plant fly ash and scrap aluminium foil in removing nickel through adsorption. Powder Technol 2019;354:792–803.
[55] Asl S, Ahmadi M, Ghiasvand M, Tardast A, Katal R. Artificial neural network (ANN) approach for modelling of Cr (VI) adsorption from aqueous solution by zeolite prepared from raw fly ash (ZFA). J Ind Eng Chem 2013;19(3):1044–55.
[56] Duan P, Yan C, Zhou W, Ren D. Development of fly ash and iron ore tailing based porous geopolymer for removal of Cu (II) from wastewater. Ceram Int 2016;42(12):13507–18.
[57] Tomasz K, Anna K, Ryszard C. Effective adsorption of lead ions using fly ash obtained in the novel circulating fluidized bed combustion technology. Microchem J 2019;145:1011–25.
[58] Adamczuk A, Kołodyńska D. Equilibrium, thermodynamic and kinetic studies on removal of chromium, copper, zinc and arsenic from aqueous solutions onto fly ash coated by chitosan. Chem Eng J 2015;274:200–12.
[59] Zhang Y, Chen Y, Kang W, Han H, Song H, Zhang C, et al. Excellent adsorption of Zn (II) using NaP zeolite adsorbent synthesized from coal fly ash via stage treatment. J Clean Prod 2020;258:120736.
[60] Qi L, Teng F, Deng X, Zhang Y, Zhong X. Experimental study on adsorption of Hg (II) with microwave-assisted alkali-modified fly ash. Powder Technol 2019;351:153–8.
[61] Gao M, Ma Q, Lin Q, Chang J, Ma H. Fabrication and adsorption properties of hybrid fly ash composites. Appl Surf Sci 2017;396:400–11.
[62] Al-Harahsheh M, Al Zboon K, Al-Makhadmeh L, Hararah M, Mahasneh M. Fly ash based geopolymer for heavy metal removal: a case study on copper removal. J Environ Chem Eng 2015;3(3):1669–77.
[63] Siyal A, Shamsuddin M, Rabat N, Zulfiqar M, Man Z, Low A. Fly ash based geopolymer for the adsorption of anionic surfactant from aqueous solution. J Clean Prod 2019;229:232–43.
[64] Al-Zboon K, Al-Harahsheh M, Hani F. Fly ash-based geopolymer for Pb removal from aqueous solution. J Hazard Mater 2011;188(1–2):414–21.
[65] Feng T, Xu J, Yu C, Cheng K, Wu Y, Wang Y, et al. Graphene oxide wrapped melamine sponge as an efficient and recoverable adsorbent for Pb (II) removal from fly ash leachate. J Hazard Mater 2019;367:26–34.
[66] Joseph I, Tosheva L, Doyle A. Simultaneous removal of Cd (II), Co (II), Cu (II), Pb (II), and Zn (II) ions from aqueous solutions via adsorption on FAU-type zeolites prepared from coal fly ash. J Environ Chem Eng 2020;8(4):103895.
[67] Darmayanti L, Kadja G, Notodarmojo S, Damanhuri E, Mukti R. Structural alteration within fly ash-based geopolymers governing the adsorption of Cu2+ from aqueous environment: effect of alkali activation. J Hazard Mater 2019;377:305–14.
[68] Kumar T, Sivasankar V, Fayoud N, Abou Oualid H, Sundramoorthy A. Synthesis and characterization of coral-like hierarchical MgO incorporated fly ash composite for the effective adsorption of azo dye from aqueous solution. Appl Surf Sci 2018;449:719–28.
[69] Asl S, Masomi M, Hosseini M, Javadian H, Ruiz M, Sastre A. Synthesis of hydrous iron oxide/aluminum hydroxide composite loaded on coal fly ash as an effective mesoporous and low-cost sorbent for Cr (VI) sorption: fuzzy logic modeling. Process Saf Environ Protect 2017;107:153–67.
[70] Wang K, Peng N, Sun J, Lu G, Chen M, Deng F, et al. Synthesis of silica-composited biochars from alkali-fused fly ash and agricultural wastes for enhanced adsorption of methylene blue. Sci Total Environ 2020;729:139055.
[71] Liu Y, Yan C, Zhao J, Zhang Z, Wang H, Zhou S, et al. Synthesis of zeolite P1 from fly ash under solvent-free conditions for ammonium removal from water. J Clean Prod 2018;202:11–22.

[72] Liu Y, Wang G, Wang L, Li X, Luo Q, Na P. Zeolite P synthesis based on fly ash and its removal of Cu (II) and Ni (II) ions. Chin J Chem Eng 2019;27(2):341–8.
[73] Darmayanti L, Notodarmodjo S, Damanhuri E. Removal of copper (II) ions in aqueous solutions by sorption onto fly ash. J Eng Technol Sci 2017;49(4):546–59.
[74] He K, Chen Y, Tang Z, H Y. Removal of heavy metal ions from aqueous solution by zeolite synthesized from fly ash. Environ Sci Pollut Res 2016;23:2778–88.
[75] Alinnor I. Adsorption of heavy metal ions from aqueous solution by fly ash. Fuel 2007;5–6(86):853–7.
[76] Yu G, Wang X, Liu J, Jiang P, You S, Ding N, et al. Applications of nanomaterials for heavy metal removal from water and soil: a review. Sustainability 2021;13(2):713.
[77] Ahmad R, Mirza A. Application of Xanthan gum/n-acetyl cysteine modified mica bionanocomposite as an adsorbent for the removal of toxic heavy metals. Groundw Sustain Dev 2018;7:101–8.
[78] Wu Y, Pang H, Liu Y, Wang X, Yu S, Fu D, et al. Environmental remediation of heavy metal ions by novel-nanomaterials: a review. Environ Pollut 2019;246:608–20.
[79] Panday K, Prasad G, Singh V. Copper (II) removal from aqueous solutions by fly ash. Water Res 1985;19(7):869–73.
[80] Xu D, Tan X, Chen C, Wang X. Adsorption of Pb(II) from aqueous solution to MX-80 bentonite: effect of pH, ionic strength, foreign ions and temperature. Appl Clay Sci 2008;41(1–2):37–46.
[81] Visa M, Isac L, Duta A. Fly ash adsorbents for multi-cation wastewater treatment. Appl Surf Sci 2012;258(17):6345–52.
[82] Wang X, Chen Z, Yang S. Application of graphene oxides for the removal of Pb(II) ions from aqueous solutions: experimental and DFT calculation. J Mol Liq 2015;211:957–64.
[83] Atun G, Hisarlı G, Kurtoglu A, Ayar N. A comparison of basic dye adsorption onto zeolitic materials synthesized from fly ash. J Hazard Mater 2011;187:562–73.
[84] Jamal H. Removal of heavy metals from acid mine drainage: a review. Int J Technol Sci Eng 2015;2:77–84.
[85] Javadian H, Ghorbani F, Tayebi H, Asl S. Study of the adsorption of Cd (II) from aqueous solution using zeolite-based geopolymer, synthesized from coal fly ash; kinetic, isotherm and thermodynamic studies. Arab J Chem 2015;8(6):837–49.
[86] Chikri R, Elhadiri N, Benchanaa M. Efficiency of sawdust as low-cost adsorbent for dyes removal. J Chem 2020;2020:1–17.
[87] Srivatsav P, Bhargav B, Shanmugasundaram V, Arun J, Gopinath K, Bhatnagar A. Biochar as an eco-friendly and economical adsorbent for the removal of colorants (dyes) from aqueous environment: a review. Water 2020;12(12):3561.
[88] López FJ, Sugita S, Tagaya M, Kobayashi T. Metakaolin-based geopolymers for targeted adsorbents to heavy metal ion separation. J Mater Sci Chem Eng 2014;2(7).
[89] Kara İ, Yilmazer D, Akar S. Metakaolin based geopolymer as an effective adsorbent for adsorption of zinc (II) and nickel (II) ions from aqueous solutions. Appl Clay Sci 2017;139:54–63.
[90] Mužek M, Svilović S, Ugrina M, Zelić J. Removal of copper and cobalt ions by fly ash-based geopolymer from solutions-equilibrium study. Desalin Water Treat 2016;57(23):10689–99.
[91] Visa M. Synthesis and characterization of new zeolite materials obtained from fly ash for heavy metals removal in advanced wastewater treatment. Powder Technol 2016;294:338–47.
[92] Wang S, Li L, Zhu Z. Solid-state conversion of fly ash to effective adsorbents for Cu removal from wastewater. J Hazard Mater 2007;139(2):254–9.
[93] Mužek M, Svilović S, Zelić J. Fly ash-based geopolymeric adsorbent for copper ion removal from wastewater. Desalin Water Treat 2014;52(13–15):2519–26.
[94] Li L, Wang S, Zhu Z. Geopolymeric adsorbents from fly ash for dye removal from aqueous solution. J Colloid Interface Sci 2006;300(1):52–9.
[95] Alouani M, Alehyen S, Achouri M, Taibi M. Removal of cationic dye methylene blue-from aqueous solution by adsorption on fly ash-based geopolymer. J Mater Environ Sci 2018;9(1):32–46.
[96] Zhang Y, Liu L. Fly ash-based geopolymer as a novel photocatalyst for degradation of dye from wastewater. Particuology 2013;11(3):353–8.
[97] Ouyang D, Zhuo Y, Hu L, Zeng Q, Hu Y, He Z. Research on the adsorption behavior of heavy metal ions by porous material prepared with silicate tailings. Minerals 2019;9:291.
[98] Ayawei N, Ebelegi A, Wankasi D. Modelling and interpretation of adsorption isotherms. J Chem 2017;2017:1–11.
[99] Lee N, Khalid H, Lee H. Adsorption characteristics of cesium onto mesoporous geopolymers containing nano-crystalline zeolites. Microporous Mesoporous Mater 2017;242:238–44.
[100] Umejuru E, Prabakaran E, Kriveshini Pillay K. Coal fly ash coated with carbon hybrid nanocomposite for remediation of cadmium (II) and photocatalytic application of the spent adsorbent for reuse. Res Mater 2020;7.
[101] Papandreou A, Stournaras C, Panias D. Copper and cadmium adsorption on pellets made from fired coal fly ash. J Hazard Mater 2007;148(3):538–47.
[102] Kumar M, Goswami L, Singh A, Sikandar M. Valorization of coal fired-fly ash for potential heavy metal removal from the single and multi-contaminated system. Heliyon 2019;5(10).

Uyiosa Osagie Aigbe is a research fellow with the Department of Mathematics and Physics, Faculty of Applied Science, Cape Peninsula University of Technology, Cape Town, South Africa. He obtained his PhD degree in Physics from the prestigious University of South Africa, Pretoria, South Africa. He is currently a member of several learned academic organizations. His research interests are in applied physics, nanotechnology, fluid dynamics, water purification processes, image processing, environmental physics, and material science. He has also served as a reviewer to numerous highly regarded journals. He has authored and co-authored several research publications.

Kingsley Eghonghon Ukhurebor is a Lecturer/Researcher presently at the Department of Physics, Edo State University Uzairue, Nigeria. He has a Ph.D. in Physics/Electronics from the University of Benin, Benin City, Nigeria. He is a Research Fellow at the West African Science Service Center on Climate Change and Adapted Land Use (WASCAL), Competence Center, Ouagadougou, Burkina Faso. He is also a prospective Postdoctoral Fellow of the World Academy of Sciences – COMSATS University Islamabad, Pakistan. He is a member of several learned academic organizations. His research interests are applied physics, climatic physics, environmental physics, telecommunication physics and material science. He serves as editor and reviewer to several reputable journals and publishers. He has authored and co-authored several publications.

Robert Birundu Onyancha is a lecturer and researcher working full-time at the department of Technical and Applied Physics, in the Technical University of Kenya (TUK). He holds a Ph.D. in Physics from the University of South Africa (UNISA). He is a registered member of various research bodies and has authored and co-authored research papers and book chapters which have been published in reputable and accredited international journals and publishers.

Otolorin Adelaja Osibote obtained her Ph.D (Medical Physics) from Escola Nacional de Saude Publica (National School of Public Health)-FIOCRUZ, Brazil. She was a postdoctoral research fellow in the Department of Nuclear Energy, Universidade Federal de Pernambuco (Federal University of Pernambuco), Brazil and in the Department of Human Biology (Biomedical Engineering) of University of Cape Town, South Africa. She was a junior research associate of the Abdus Salam International Center for Theoretical Physics from 2002 to 2006. Dr. Osibote assumed a faculty position in the Department of Physics, Olabisi Onabanjo University in 1995 and presently in the Department of Mathematics and Physics, Cape Peninsula University of Technology, South Africa. She has carried out research on several areas including irradiation of foodstuffs, quality assurance in diagnostic radiology, developments of algorithms for automated focusing of a microscope for the detection of tuberculosis and measurement of heavy metals and radioactivity in food and environmental fields.

Handoko Darmokoesoemo received a doctoral degree in Mathematics and Natural Science from Airlangga University. His current research fields are dealing with adsorbents (biosorbents) for adsorption of heavy metals and dyes. He is the author or co-author of more than 50 papers on national and international journals and conference proceedings. He is currently a Lecturer in Department of Chemistry, Faculty of Science and Technology, Airlangga University, Indonesia.

Heri Septya Kusuma received a bachelor's degree in Chemistry from Airlangga University, a master's degree in Chemical Engineering from Institut Teknologi Sepuluh Nopember and a doctoral degree in Chemical Engineering from Institut Teknologi Sepuluh Nopember. His current research fields are dealing with adsorbents (biosorbents) for adsorption of heavy metals and dyes; natural products; biofuels; and optimization (modeling). He is the author or co-author of more than 90 papers on national and international journals and conference proceedings. He also serves as editor and reviewer to several reputable journals and publishers. He is currently a Lecturer in Department of Chemical Engineering, Faculty of Industrial Technology, Universitas Pembangunan Nasional "Veteran" Yogyakarta, Indonesia.